# X-ray bursts studies using indirect methods

**Nicolas de Séréville** (nicolas.de-sereville@ijclab.in2p3.fr)
Laboratoire de Physique des 2 Infinis Irène Joliot Curie
Université Paris Saclay

# Outline

1. Generalities

2. Break out of the hot CNO cycle

   a) The $^{15}O(\alpha,\gamma)^{19}Ne$ reaction

   b) The $^{18}Ne(\alpha,p)^{21}Na$ reaction

3. The $\alpha$p-process and the $^{35}K(p,\gamma)^{36}Ca$ reaction

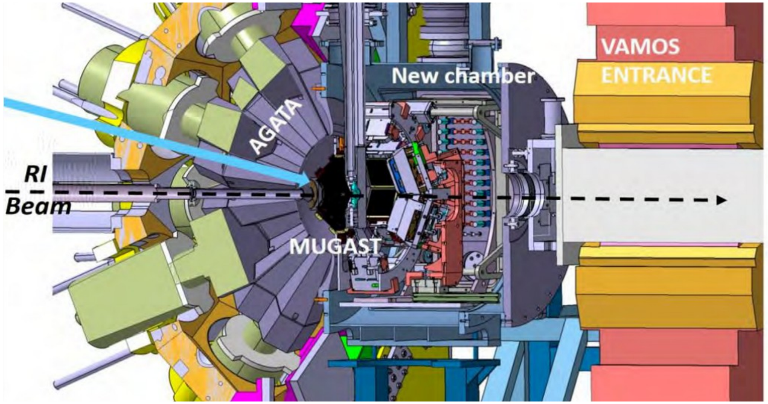


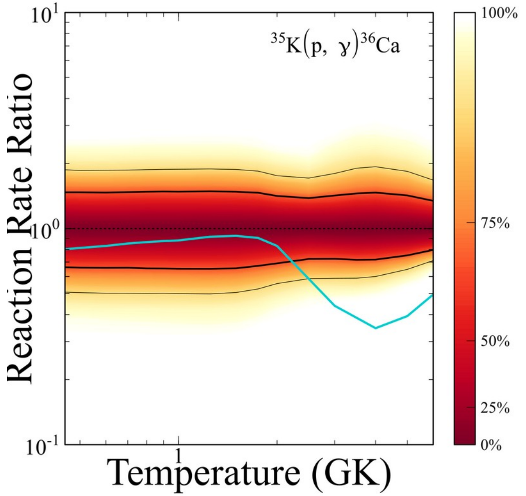

# Outline

1. Generalities
2. Break out of the hot CNO cycle
   a) The $^{15}O(\alpha,\gamma)^{19}Ne$ reaction
   b) The $^{18}Ne(\alpha,p)^{21}Na$ reaction
3. The $\alpha$p-process and the $^{35}K(p,\gamma)^{36}Ca$ reaction

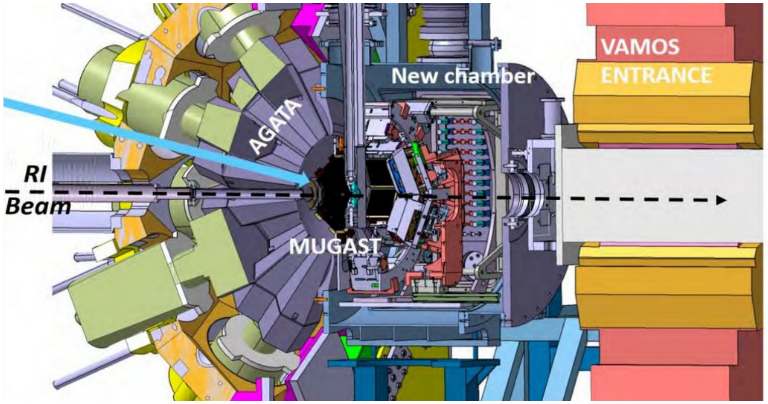


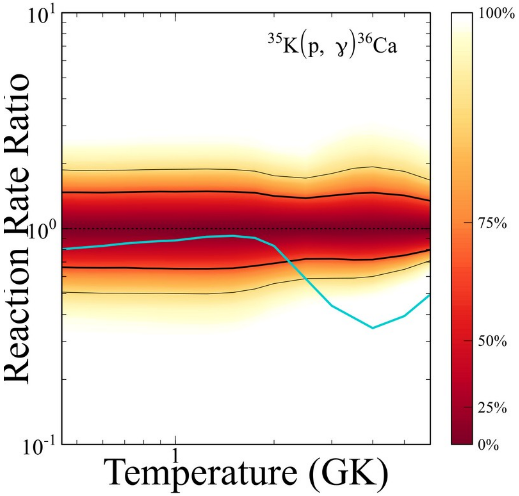

# Type I X-ray burst in a nutshell

Thermonuclear runaway at the surface of a neutron star (NS) in a close binary system

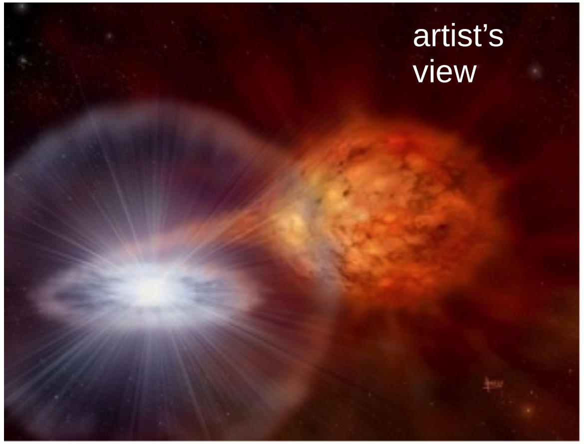


Recurrent flashes [e.g. 4U/MXB 1820-30]

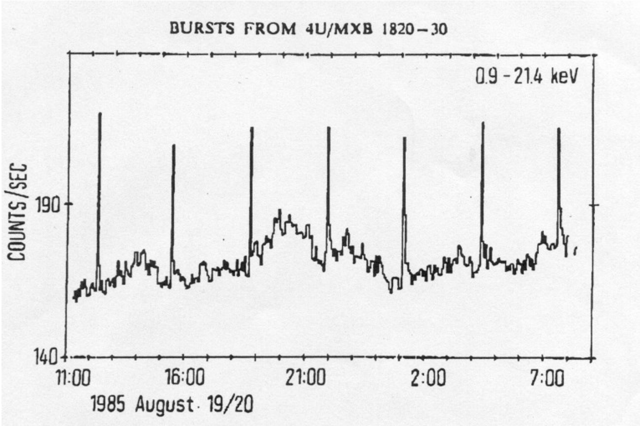


Precision era for X-ray observations

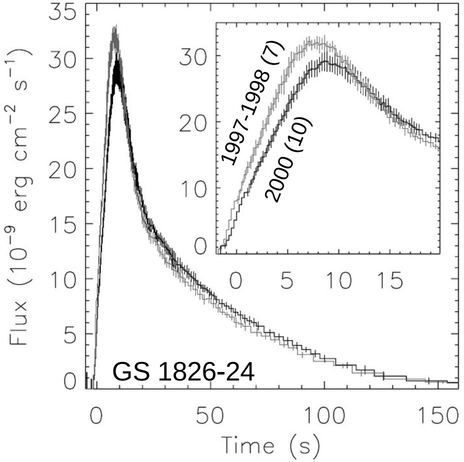


D. K. Galloway+ (2004)

Type I X-ray outbursts

- Very fast rise times: 2 – 10 s
- $L_{peak}$ ~ $10^{38}$ erg $s^{-1}$
  (ccSN $L_{peak}$ ~ $10^{51}$ erg.$s^{-1}$)
- Short duration: 10 – 100 s
- Recurence time: ~ hours – days
- Mass ejected: maybe (?)

Y. Herrera+ (2023)

Understand the luminosity profile (one of the most important challenge)

- Sensitive to NS spin frequency (oscillations in rise part of light curve) S. Bhattacharyya+ (2007)
- Sensitive to NS mass-radius relation (tail of light curve) J. Nattila+ (2017)
- **Very sensitive to nuclear inputs**

# Nuclear network and uncertainties

- Main nuclear path far from the valley of stability
  → ~ 300 – 500 relevant nuclides
  → several thousands reactions

- End point of nucleosynthesis: Sn–Sb–Te cycle
  Schatz+ 2001

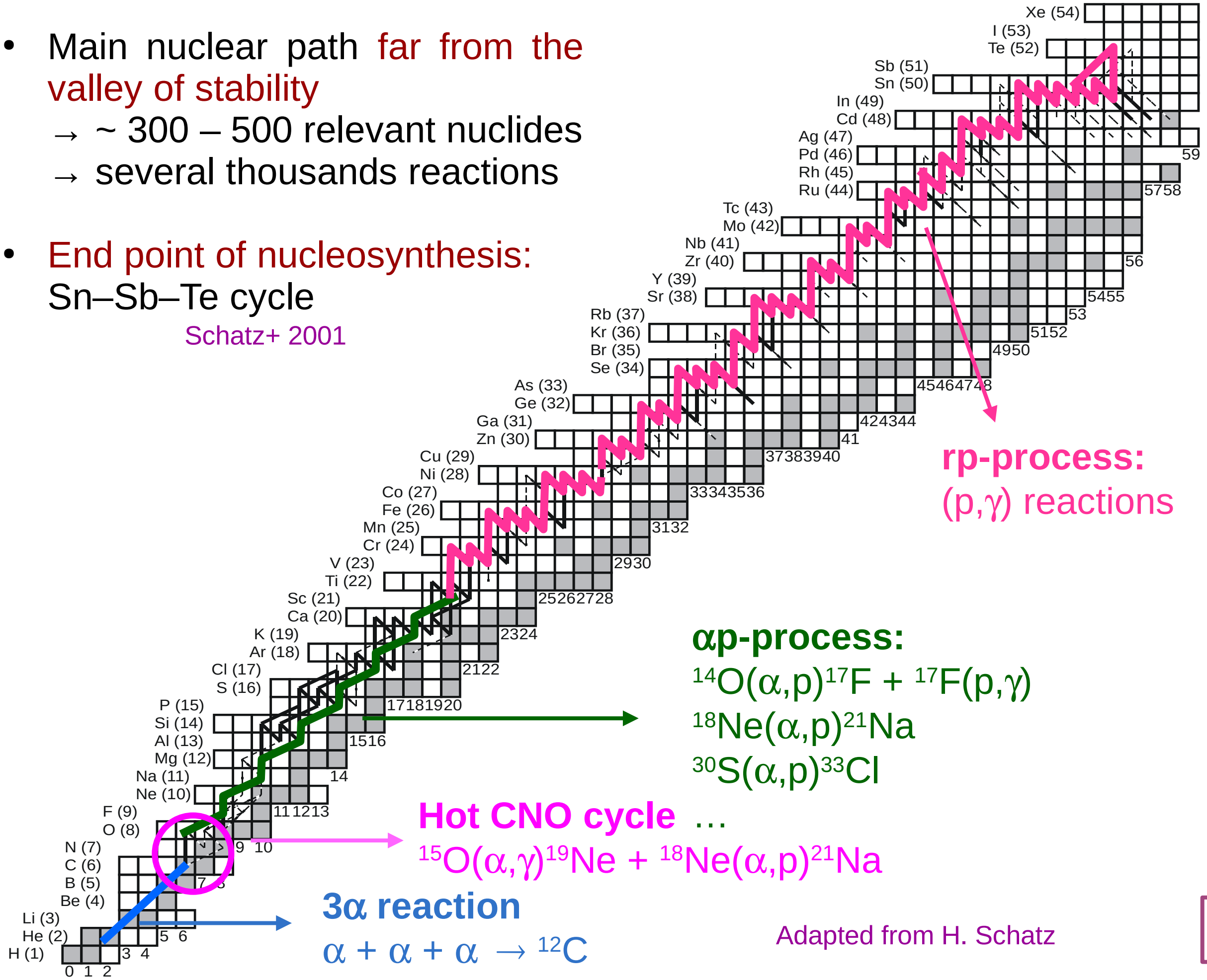


**rp-process:**
(p,γ) reactions

**αp-process:**
$^{14}O(\alpha,p)^{17}F$ + $^{17}F(p,\gamma)$
$^{18}Ne(\alpha,p)^{21}Na$
$^{30}S(\alpha,p)^{33}Cl$

**Hot CNO cycle** …
$^{15}O(\alpha,\gamma)^{19}Ne$ + $^{18}Ne(\alpha,p)^{21}Na$

**3α reaction**
$\alpha + \alpha + \alpha \rightarrow {}^{12}C$

Adapted from H. Schatz

## Nuclear Physics inputs

- Mass measurements along *rp*-process path
- Key reactions
- …

## Sensitivity studies

Parikh+ ApJ (2013), Meisel+ ApJ (2019)
Cyburt+ ApJ (2016)

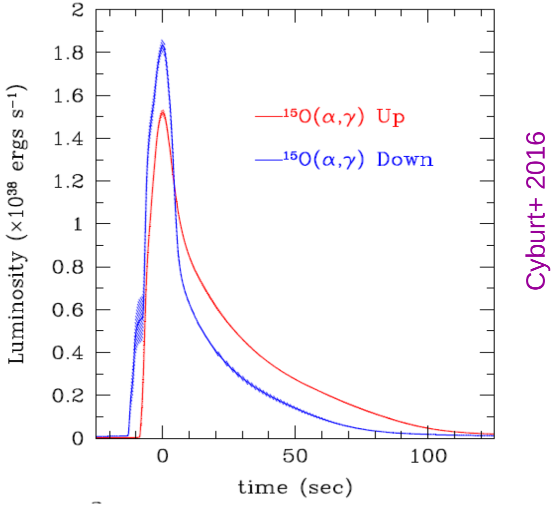


Only a few tens of key reactions are important

# Cross-section determination: experimental strategies

## Cross section

$$\sigma(E) = \frac{1}{E} S(E) \exp(-2\pi\eta)$$

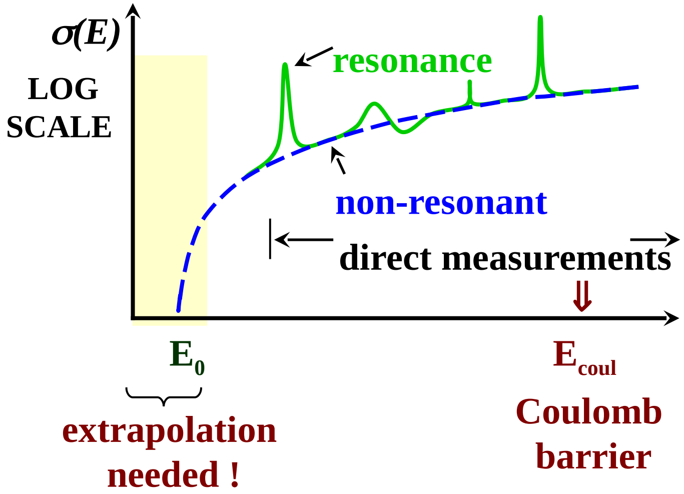


## Astrophysical *S*-factor

$$S(E) = E\,\sigma(E) \exp(2\pi\eta)$$

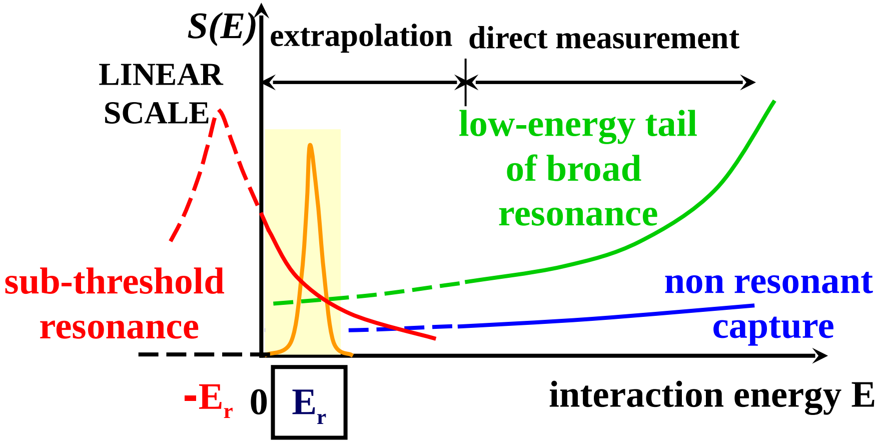


Problems with EXTRAPOLATION !

- Measurement of cross section at higher energies and extrapolation to astrophysical energies $E_0$
  → direct measurement approach
- Determination of resonant state properties ($E_R$, partial widths $\Gamma_i$, $J^\pi$)
  → indirect measurement approach

# Direct measurements: requirements and challenges

Low cross section → low yields → poor signal-to-noise ratio

## Sources of background

- Beam induced
  - Reactions with impurities in the target
  - Reactions on beam collimators/apertures

- Non beam-induced
  - Interaction from cosmic muons with detection setup
  - Charged particles / $\gamma$-rays from natural background
  - Neutron induced reactions

**see lectures from M. Heine and A. Bonhomme**

## Requirements & challenges → Improving signal-to-noise ratio

- Improving signal
  - Very long measurements (weeks, months…)
  - High beam intensities: heating effects on target (limitation)
  - Thicker targets (?): exponential drop of the cross section
  - High detection efficiency

- Reducing noise/background
  - Ultra pure targets: difficult
  - Dedicated experimental setup →
    - Coincidence measurements (STELLA…)
    - Recoil mass separator (DRAGON…)
    - Underground laboratory (LUNA, Felsenkeller...)

# Indirect measurements

Cross-section of astrophysical interest not measured directly

## Main idea:

- Perform experiments above the Coulomb barrier at high energy (~ few – 10's of MeV/u)
  → higher cross sections than for direct measurements

## Pros and Cons:

- ✔ Experimental conditions are relatively less constraining than for direct measurement (not necessarily true with RIB studies)

- ✖ Results are model dependent
- Results depend on the uncertainties relative to the different model parameters

- Examples of indirect methods:
  - **Transfer reactions**, Asymptotic Normalization Coefficient (ANC) method, Trojan Horse Method (THM), surrogate method, Coulomb dissociation...

**see lecture from F. Hammache**

# Outline

1. Generalities

2. Break out of the hot CNO cycle

   a) The $^{15}O(\alpha,\gamma)^{19}Ne$ reaction

   b) The $^{18}Ne(\alpha,p)^{21}Na$ reaction

3. The $\alpha$p-process and the $^{35}K(p,\gamma)^{36}Ca$ reaction

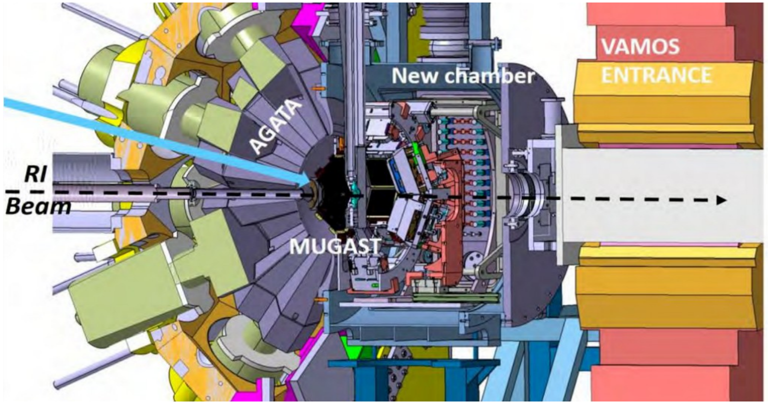


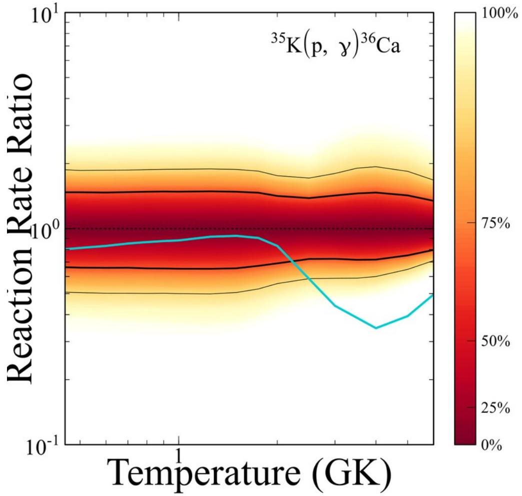

# Hot-CNO cycle breakout reactions

**$^{15}O(\alpha,\gamma)^{19}Ne$:** first break out reaction

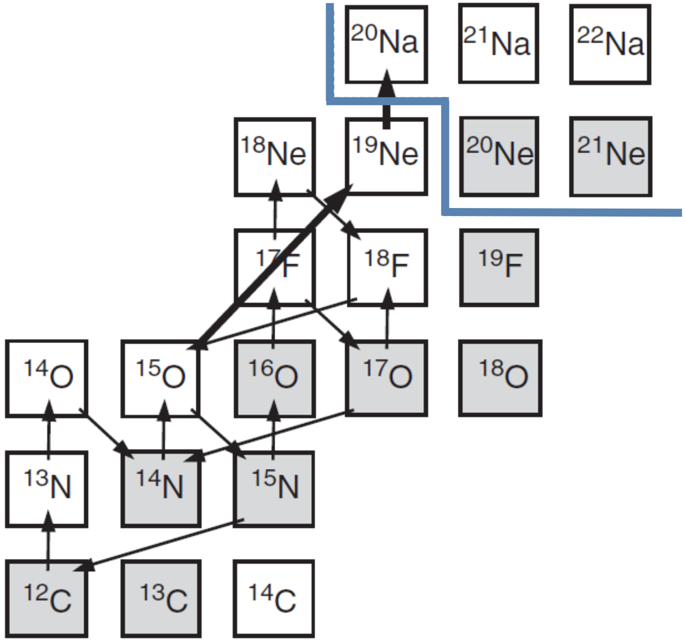


- **$^{15}O(\alpha,\gamma)^{19}Ne$** much slower than $^{19}Ne(p,\gamma)^{20}Na$

# Hot-CNO cycle breakout reactions

**$^{15}O(\alpha,\gamma)^{19}Ne$:** first break out reaction

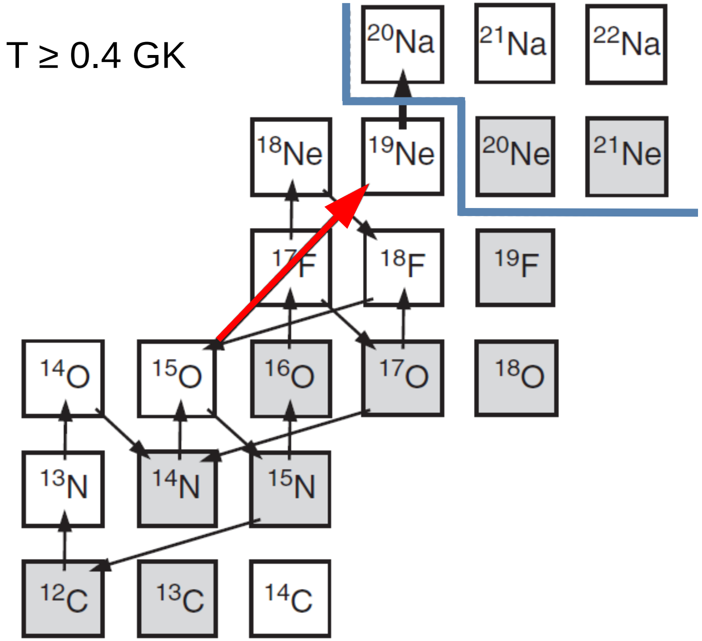


- **$^{15}O(\alpha,\gamma)^{19}Ne$** much slower than $^{19}Ne(p,\gamma)^{20}Na$

# Hot-CNO cycle breakout reactions

**$^{15}$O(α,γ)$^{19}$Ne:** first break out reaction

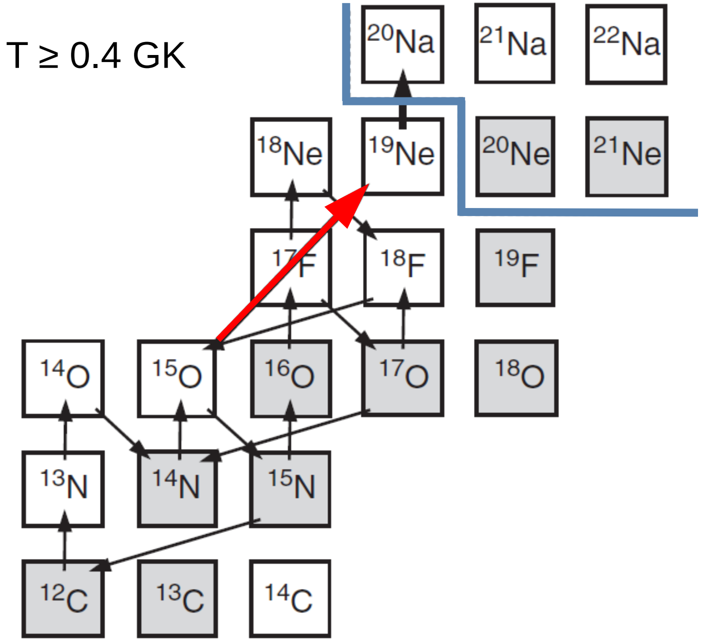


- **$^{15}$O(α,γ)$^{19}$Ne** much slower than $^{19}$Ne(p,γ)$^{20}$Na

**$^{18}$Ne(α,p)$^{21}$Na:** break out reaction at higher temperature

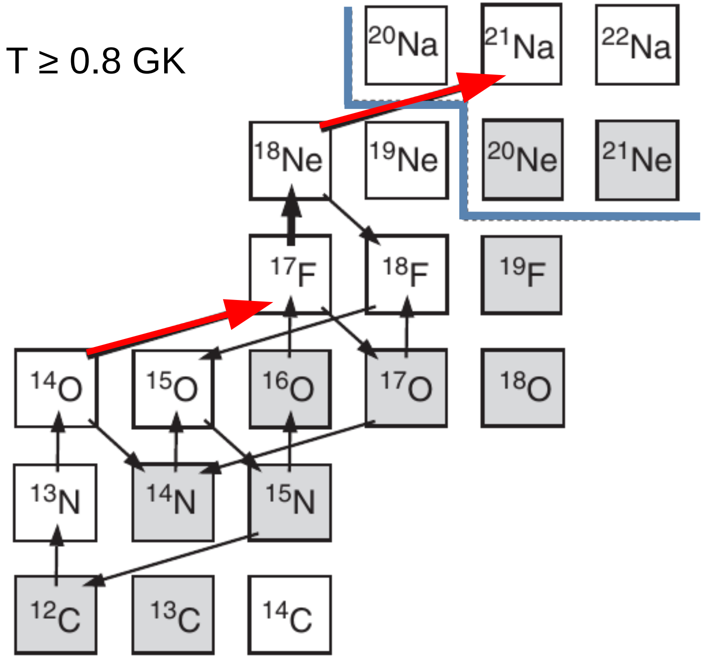


- **$^{18}$Ne(α,p)$^{21}$Na** slower than $^{14}$O(α,p)$^{17}$F and $^{17}$F(p,γ)$^{18}$Ne

# $^{15}O(\alpha,\gamma)^{19}Ne$: $^{19}Ne$ and $^{19}F$ spectroscopy

## Useful information:

- $^{15}O + \alpha \rightarrow {}^{19}Ne + \gamma$
  (1/2-) (0+)

- Compound nucleus: $^{19}Ne$
- $\ell_\alpha = 0$ resonances: $J = 1/2^-$
- $\ell_\alpha = 1$ resonances: $J = 3/2^+$
- $S_p = 6.410$ MeV; $S_\alpha = 3.528$ MeV

## Gamow window:

- $T_9 = 0.4 \rightarrow E_0 = 617$ keV; $\Delta = 337$ keV
- $T_9 = 1 \rightarrow E_0 = 1137$ keV; $\Delta = 723$ keV
- Center of mass: [450 keV; 1500 keV]
- $^{19}Ne$ excitation energy: [3.980 MeV; 5.027 MeV]

## Mirror nuclei: $^{19}Ne \leftrightarrow {}^{19}F$

- Swapped number of protons and neutrons

## Analog states:

- Similar properties ($J^\pi$, $\Gamma_i$ ...)

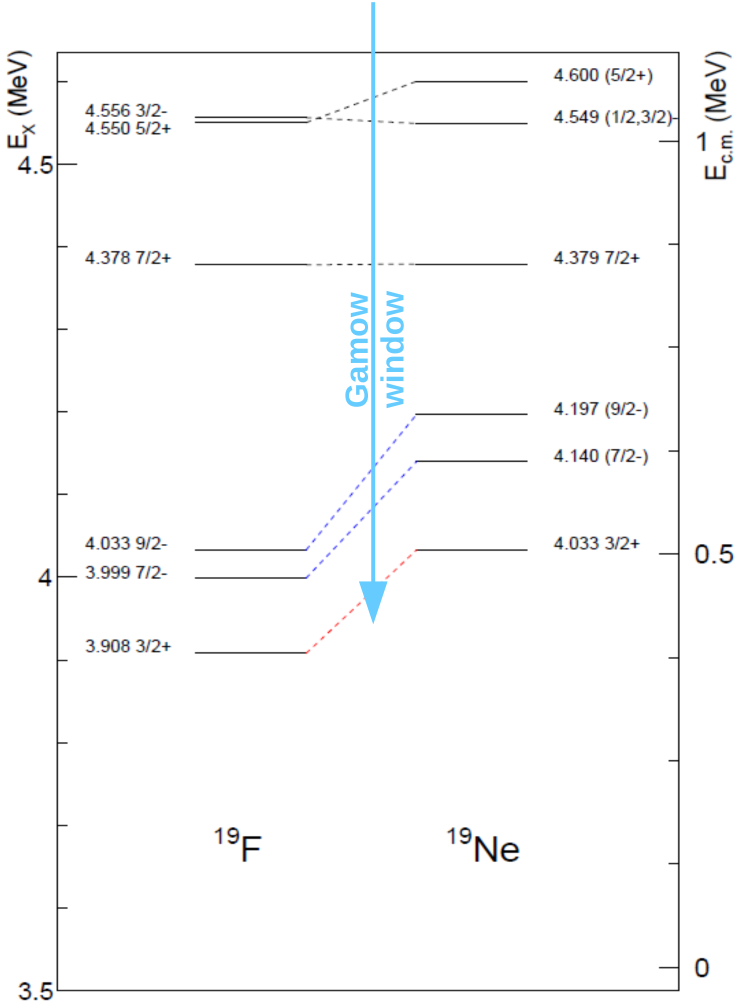

# $^{15}O(\alpha,\gamma)^{19}Ne$: what to measure and how?

## Thermonuclear reaction rate

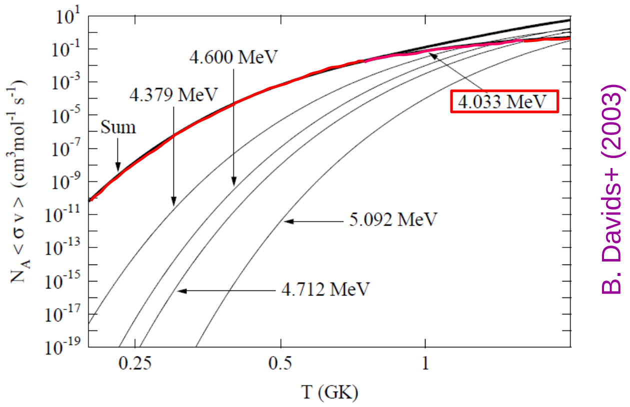


- Dominant state at $E_x$ = 4.033 MeV
  ($E_R$ = 505 keV; $J^\pi$ = 3/2$^+$; $\ell_\alpha$ = 1)

## Narrow resonance case

- $\mathcal{N}_A \langle \sigma v \rangle \propto \omega\gamma \; e^{-E_R/kT}$
- $\omega\gamma = 0.5 \times (2J_R + 1) \dfrac{\Gamma_\alpha \Gamma_\gamma}{\Gamma}$
- Close to $\alpha$-particle threshold (case of $E_x$ = 4.033 MeV state)

  → $\Gamma_\alpha \ll \Gamma_\gamma \;\Rightarrow\; \Gamma = \Gamma_\alpha + \Gamma_\gamma \approx \Gamma_\gamma$

  $$\omega\gamma \approx 0.5 \times (2J_R + 1)\,\Gamma_\alpha$$

  → resonance strength proportional to the $\alpha$-particle width (smaller partial width)

# $^{15}O(\alpha,\gamma)^{19}Ne$: what to measure and how?

## Thermonuclear reaction rate

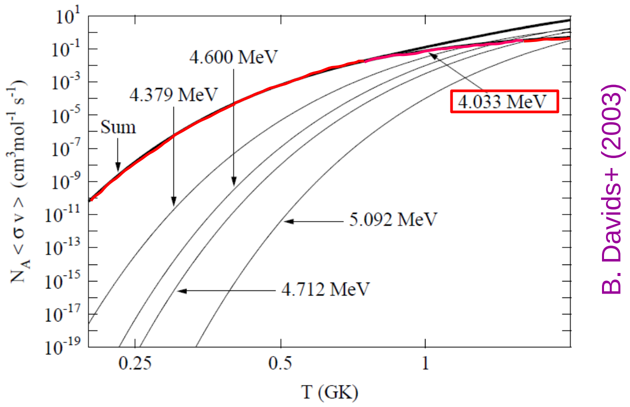


- Dominant state at $E_x$ = 4.033 MeV
  ($E_R$ = 505 keV; $J^\pi = 3/2^+$; $\ell_\alpha = 1$)

## Narrow resonance case

- $\mathcal{N}_A \langle \sigma v \rangle \propto \omega\gamma \; e^{-E_R/kT}$
- $\omega\gamma = 0.5 \times (2J_R + 1) \dfrac{\Gamma_\alpha \Gamma_\gamma}{\Gamma}$
- Close to $\alpha$-particle threshold (case of $E_x$ = 4.033 MeV state)

→ $\Gamma_\alpha \ll \Gamma_\gamma \Rightarrow \Gamma = \Gamma_\alpha + \Gamma_\gamma \approx \Gamma_\gamma$

$$\omega\gamma \approx 0.5 \times (2J_R + 1)\, \Gamma_\alpha$$

→ resonance strength proportional to the $\alpha$-particle width (smaller partial width)

## Experimental approaches

- Direct measurement: requires ~ $10^{10}$ pps of low-energy $^{15}O$ RIB [not available]
- Indirect approach: $\Gamma_\alpha = \dfrac{\Gamma_\alpha}{\Gamma} \times \Gamma = B_\alpha \times \Gamma$
  - Measurement of $\alpha$ branching ratio $B_\alpha$
  - Measurement of state lifetime $\tau \propto 1/\Gamma$
- Transfer reaction approach: $\Gamma_\alpha = C^2 S_\alpha \times \Gamma_\alpha^{s.p.}$
  - Measurement of $\alpha$ spectroscopic factor $C^2 S_\alpha$

# Doppler-Shift Attenuation Method



DSAM: Doppler-Shift Attenuation Method
→ lifetime of state inferred from the measured decaying γ-ray energy distribution

## Doppler effect

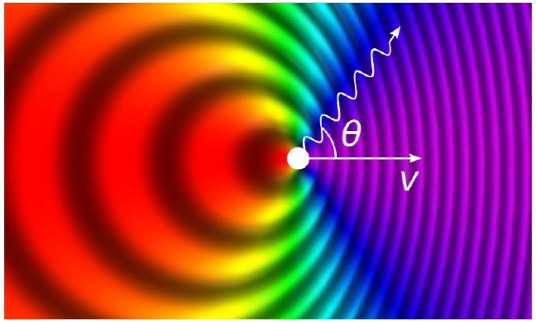


- Detected γ-ray energy ($E_\gamma$) depends on the speed ($v$) of the nucleus at emission time and on the angle (θ) between the observer and the emitting nucleus direction
- $E_\gamma = E_\gamma^0 \left(1 + \frac{v}{c} cos(\theta)\right)$

## DSAM principle

- Population of state of interest through a chosen nuclear reaction
- Slowing and stopping of recoil nucleus
- γ-ray emission at range of velocities

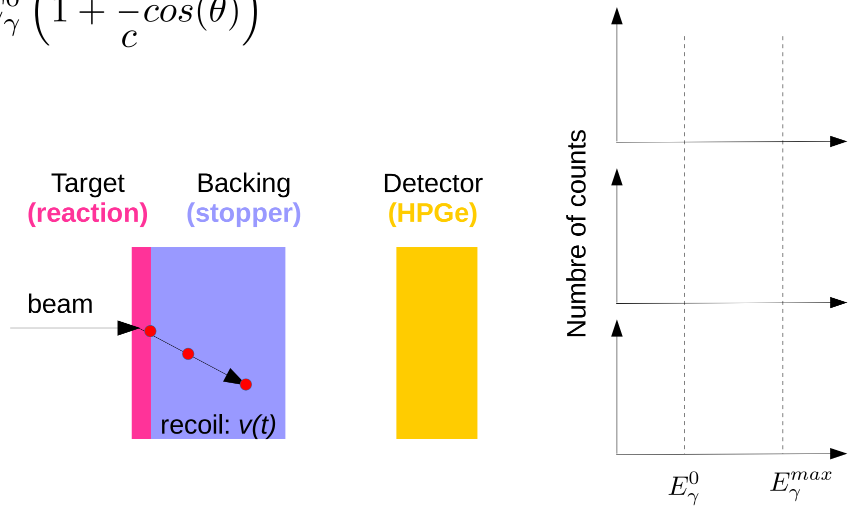

# Doppler-Shift Attenuation Method



DSAM: Doppler-Shift Attenuation Method
→ lifetime of state inferred from the measured decaying γ-ray energy distribution

## Doppler effect

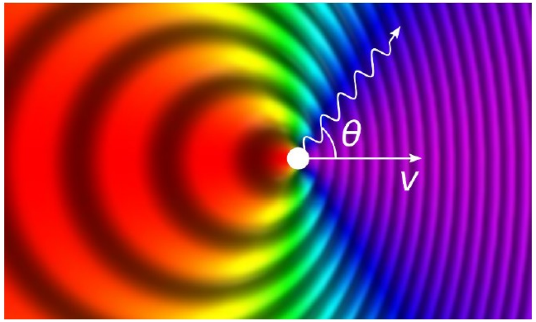


- Detected γ-ray energy ($E_\gamma$) depends on the speed ($v$) of the nucleus at emission time and on the angle (θ) between the observer and the emitting nucleus direction
- $E_\gamma = E_\gamma^0 \left(1 + \frac{v}{c} cos(\theta)\right)$

## DSAM principle

- Population of state of interest through a chosen nuclear reaction
- Slowing and stopping of recoil nucleus
- γ-ray emission at range of velocities

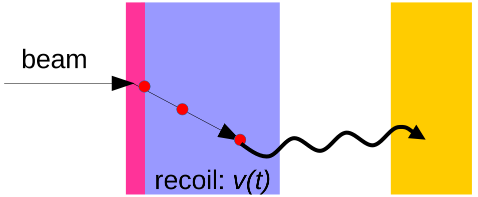


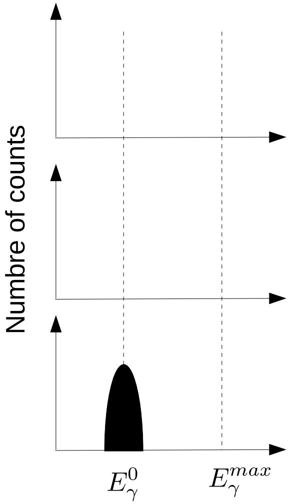


Fully stopped
$\tau > \tau_{stopping}$

# Doppler-Shift Attenuation Method



DSAM: Doppler-Shift Attenuation Method
→ lifetime of state inferred from the measured decaying γ-ray energy distribution

## Doppler effect

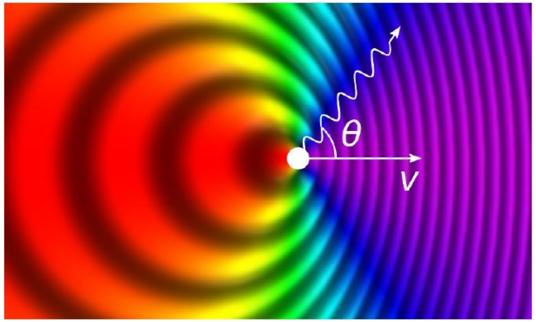


- Detected γ-ray energy ($E_\gamma$) depends on the speed ($v$) of the nucleus at emission time and on the angle (θ) between the observer and the emitting nucleus direction
- $E_\gamma = E_\gamma^0 \left(1 + \frac{v}{c} cos(\theta)\right)$

## DSAM principle

- Population of state of interest through a chosen nuclear reaction
- Slowing and stopping of recoil nucleus
- γ-ray emission at range of velocities

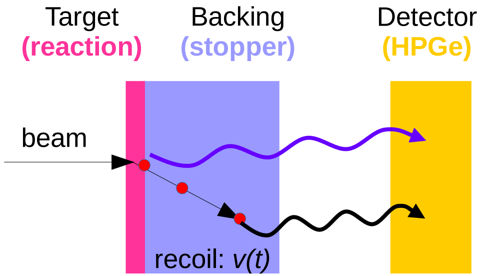


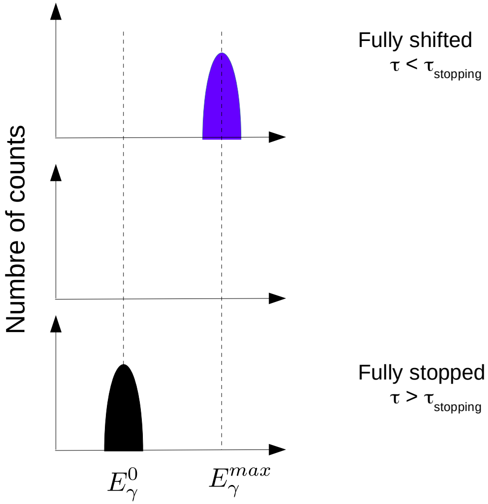

# Doppler-Shift Attenuation Method



DSAM: Doppler-Shift Attenuation Method
→ lifetime of state inferred from the measured decaying γ-ray energy distribution

## Doppler effect

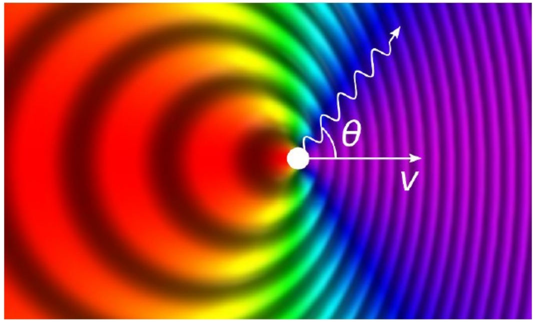


- Detected γ-ray energy ($E_\gamma$) depends on the speed ($v$) of the nucleus at emission time and on the angle (θ) between the observer and the emitting nucleus direction
- $$E_\gamma = E_\gamma^0 \left(1 + \frac{v}{c} cos(\theta)\right)$$

## DSAM principle

- Population of state of interest through a chosen nuclear reaction
- Slowing and stopping of recoil nucleus
- γ-ray emission at range of velocities

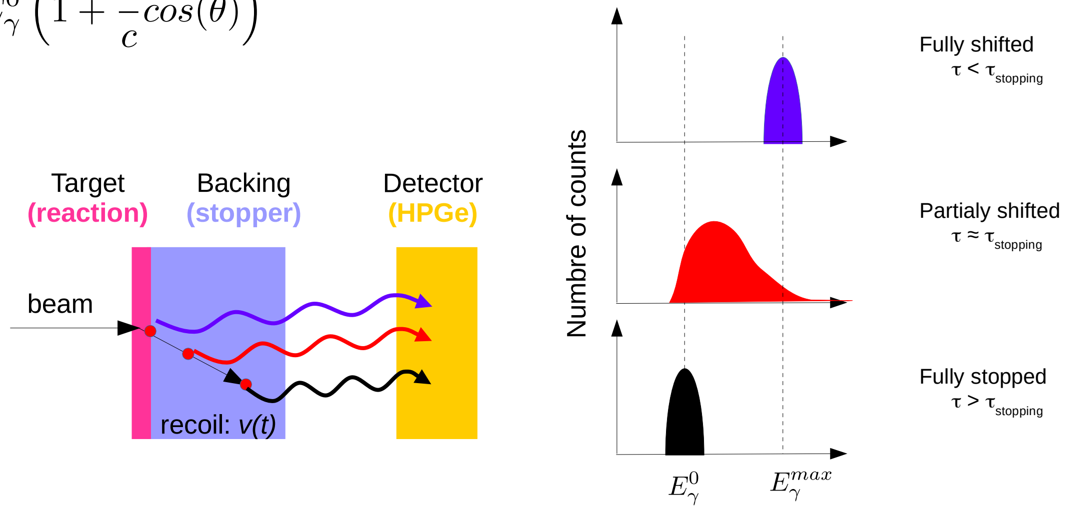

# Doppler-Shift Attenuation Method



DSAM: Doppler-Shift Attenuation Method
→ lifetime of state inferred from the measured decaying γ-ray energy distribution

## Doppler effect

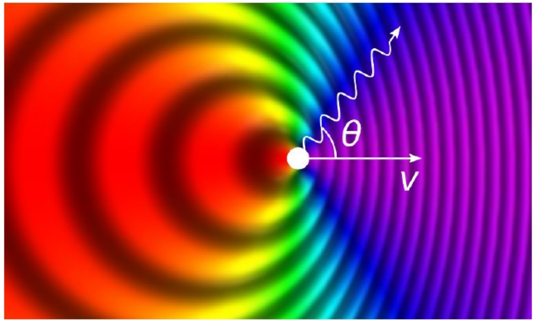


- Detected γ-ray energy ($E_\gamma$) depends on the speed ($v$) of the nucleus at emission time and on the angle (θ) between the observer and the emitting nucleus direction
- $E_\gamma = E_\gamma^0 \left(1 + \frac{v}{c} cos(\theta)\right)$

## DSAM principle

- Population of state of interest through a chosen nuclear reaction
- Slowing and stopping of recoil nucleus
- γ-ray emission at range of velocities

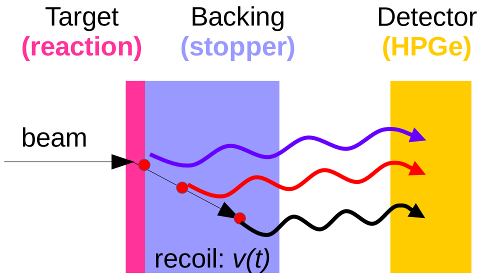


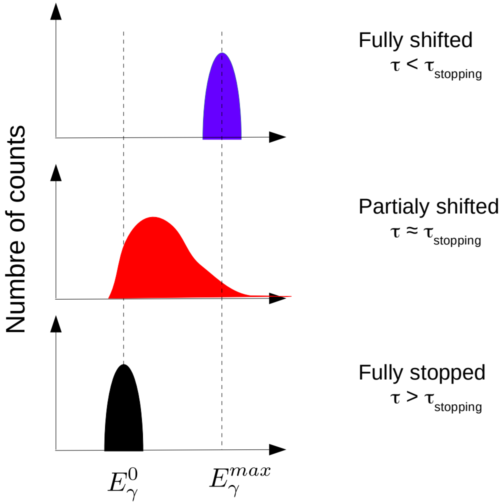


γ-ray line shape is sensitive to the lifetime of nuclear states

# Lifetime measurement of the 4033 keV state



R. Kanungo+ (2006)

## Experimental set-up

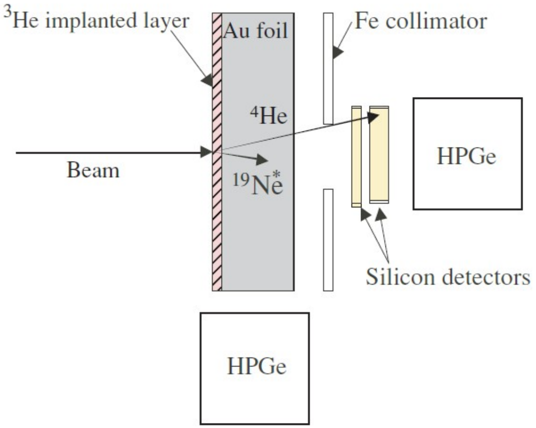


- $^{3}He(^{20}Ne,\alpha)^{19}Ne^{*}$ @ 34 MeV [TRIUMF]
- $^{3}He$ ($6x10^{17}$ at.cm$^{-2}$) implanted in 12.5 μm Au foil
- 2 HPGe at 0° and 90°
- $\Delta E$ (25 μm) - $E$ (500 μm) silicon detectors telescope

→ coincidence α-γ measurement

# Lifetime measurement of the 4033 keV state



R. Kanungo+ (2006)

## Experimental set-up

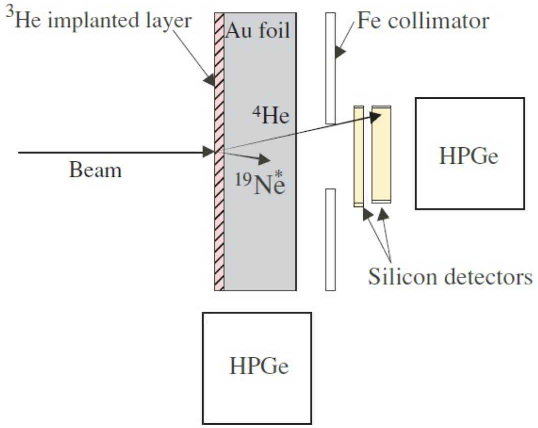


- $^{3}$He($^{20}$Ne,$\alpha$)$^{19}$Ne* @ 34 MeV [TRIUMF]
- $^{3}$He (6x10$^{17}$ at.cm$^{-2}$) implanted in 12.5 $\mu$m Au foil
- 2 HPGe at 0° and 90°
- $\Delta E$ (25 $\mu$m) - $E$ (500 $\mu$m) silicon detectors telescope

→ coincidence $\alpha$-$\gamma$ measurement

## Reaction channel identification

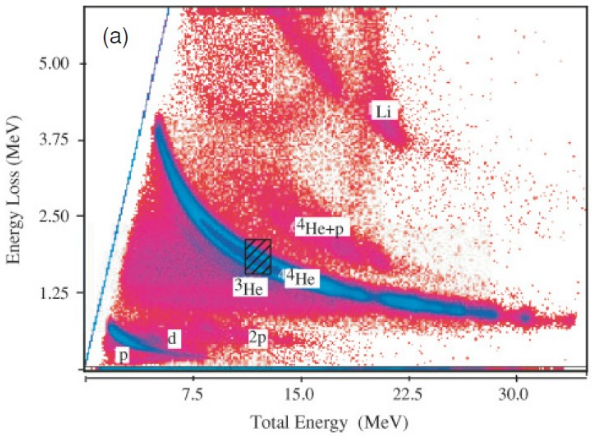


- Wide range of $\alpha$-particle energy

→ fusion-evaporation $^{20}$Ne + $^{12}$C (contaminant)

- Hatched area [$E_\alpha$ = 11 – 13 MeV]

→ $\alpha$-particles corresponding to population of 4.033 MeV state

# Lifetime measurement of the 4033 keV state



R. Kanungo+ (2006)

## Experimental set-up

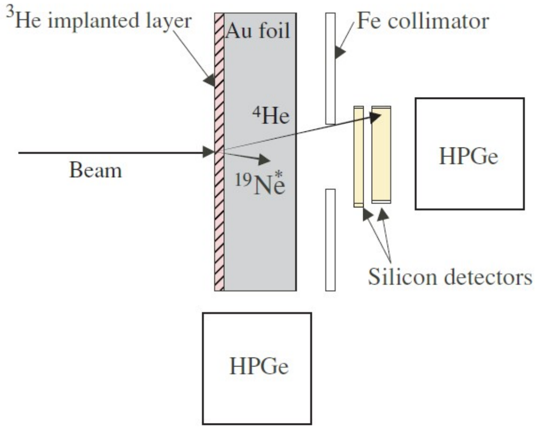


- $^3$He($^{20}$Ne,α)$^{19}$Ne* @ 34 MeV [TRIUMF]
- $^3$He (6x10$^{17}$ at.cm$^{-2}$) implanted in 12.5 μm Au foil
- 2 HPGe at 0° and 90°
- Δ$E$ (25 μm) - $E$ (500 μm) silicon detectors telescope

→ coincidence α-γ measurement

## Reaction channel identification

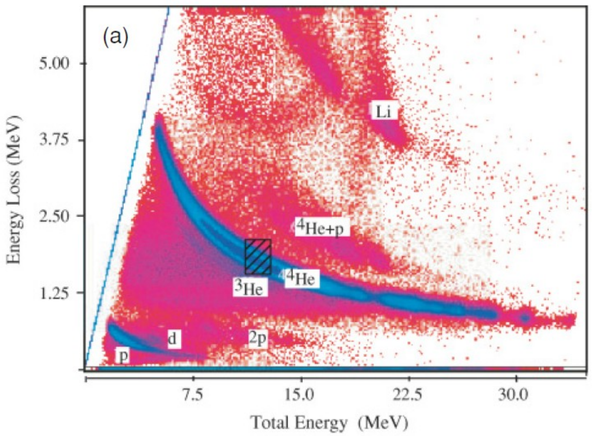


- Wide range of α-particle energy

→ fusion-evaporation $^{20}$Ne + $^{12}$C (contaminant)

- Hatched area [$E_\alpha$ = 11 – 13 MeV]

→ α-particles corresponding to population of 4.033 MeV state

## $E_\gamma$ = 4033 keV line shape

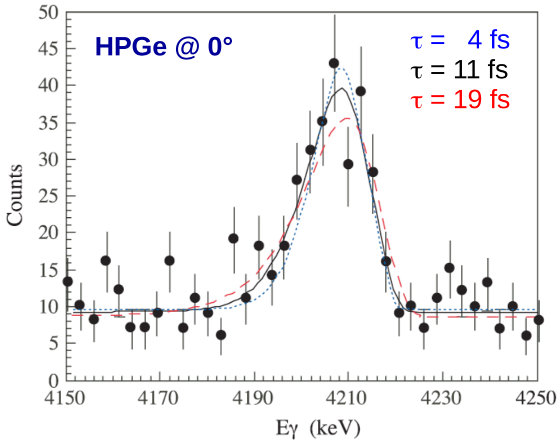


- $\tau = 11^{+4}_{-3}$ fs $(1\sigma)$
- Good agreement with existing works:
  - $\tau = 13^{+9}_{-6}$ fs $(1\sigma)$
    W. P. Tan+ (2005)
  - $\tau = 6.9^{+1.5}_{-1.5} \pm 0.7$ fs $(1\sigma)$
    S. Mythili+ (2008)

# How to determine branching ratios



W. P. Tan+ (2007, 2009)

α-particle branching ratio $B_\alpha = \frac{\Gamma_\alpha}{\Gamma}$ is the probability for an unbound state to decay through α emission

Experimentally: coincidence measurement

- Detector close to 0° (silicon, spectrometer…)
  - Detection of particles allowing the identification of the reaction and states of interest (2-body kinematics)
    → “single” events $N_{singles}$
  - Strong alignment of magnetic substates
- Silicon detector array (stripped) surrounding the target
  - Detection of decaying particles
    → “coincident” events $N_{coinc}$
  - Angular correlation measurement
    → use to determine the number of decay $N_{decays}$
- Branching ratios $B_\alpha = \frac{N_{decays}}{N_{singles}}$

# How to determine branching ratios



W. P. Tan+ (2007, 2009)

α-particle branching ratio $B_\alpha = \frac{\Gamma_\alpha}{\Gamma}$ is the probability for an unbound state to decay through α emission

Experimentally: coincidence measurement

- Detector close to 0° (silicon, spectrometer…)
  - Detection of particles allowing the identification of the reaction and states of interest (2-body kinematics)
    → "single" events $N_{singles}$
  - Strong alignment of magnetic substates
- Silicon detector array (stripped) surrounding the target
  - Detection of decaying particles
    → "coincident" events $N_{coinc}$
  - Angular correlation measurement
    → use to determine the number of decay $N_{decays}$
- Branching ratios $B_\alpha = \frac{N_{decays}}{N_{singles}}$

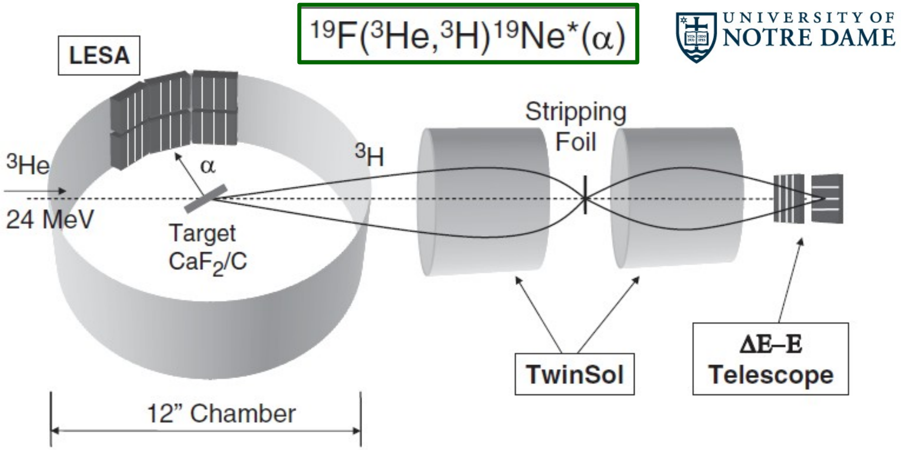


Challenge: low-energy α-particle (< 1 MeV)
- Thin target, thin detector dead layer, low electronic threshold

# Branching ratio results



W. P. Tan+ (2007, 2009)

Triton energy spectrum (single)

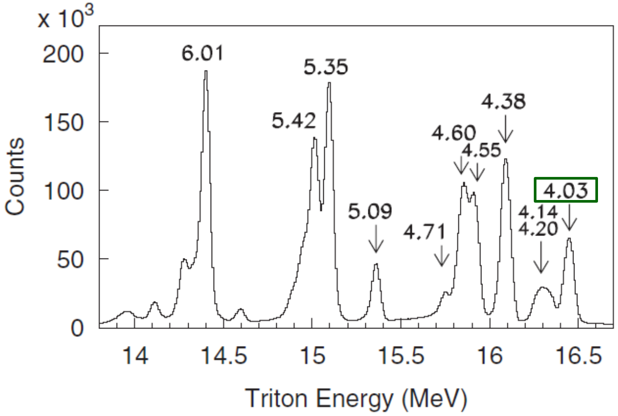

# Branching ratio results



W. P. Tan+ (2007, 2009)

## Triton energy spectrum (single)

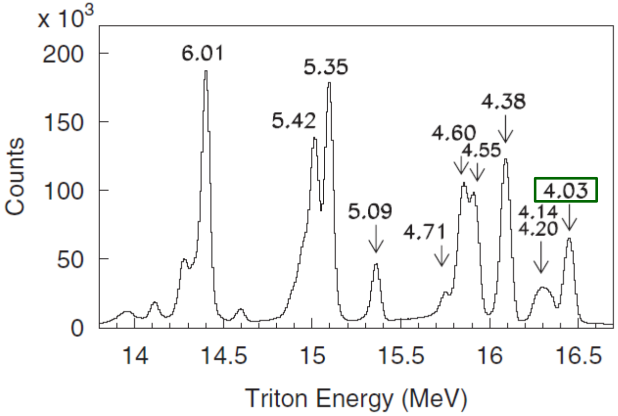


## α-particle energy spectrum (α-t coincidence)

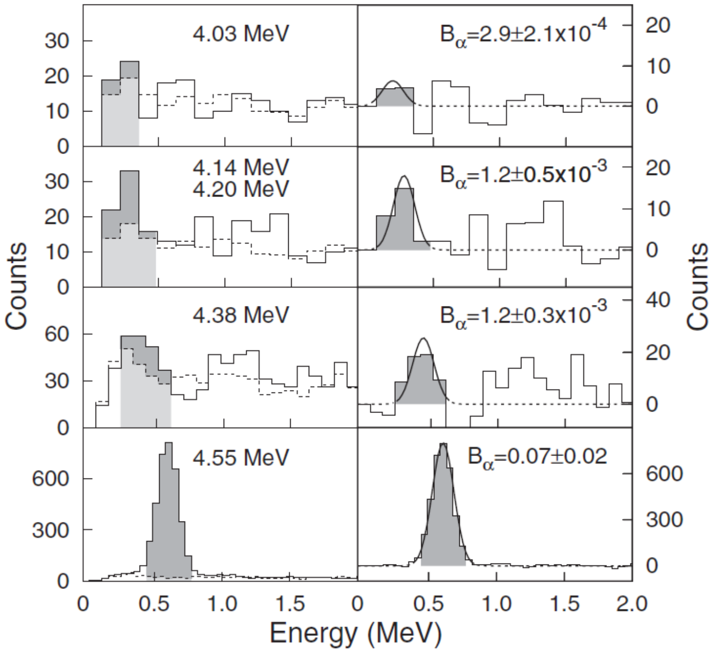


Left:
- Solid (all coincidences)
- Dashed (background)

Right:
- Backgound subtracted

# Branching ratio results



W. P. Tan+ (2007, 2009)

## Triton energy spectrum (single)

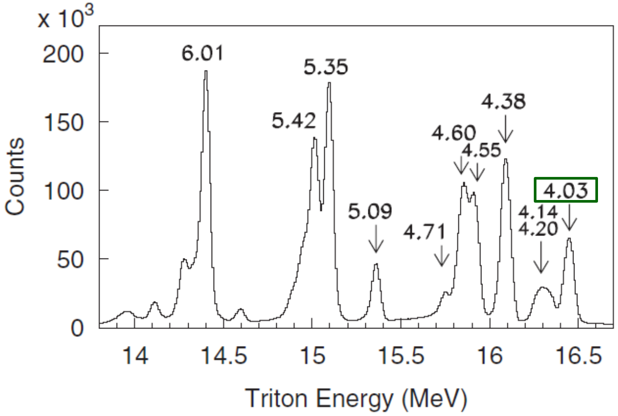


## α-t angular correlation

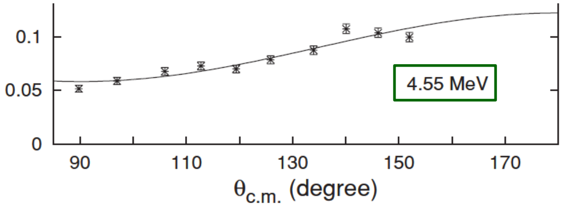


$$W(\theta_{c.m.}) = \frac{1}{4\pi}\sum_{k=0}^{k_{max}} a_{2k}P_{2k}(cos(\theta_{c.m.}))$$

## α-particle energy spectrum (α-t coincidence)

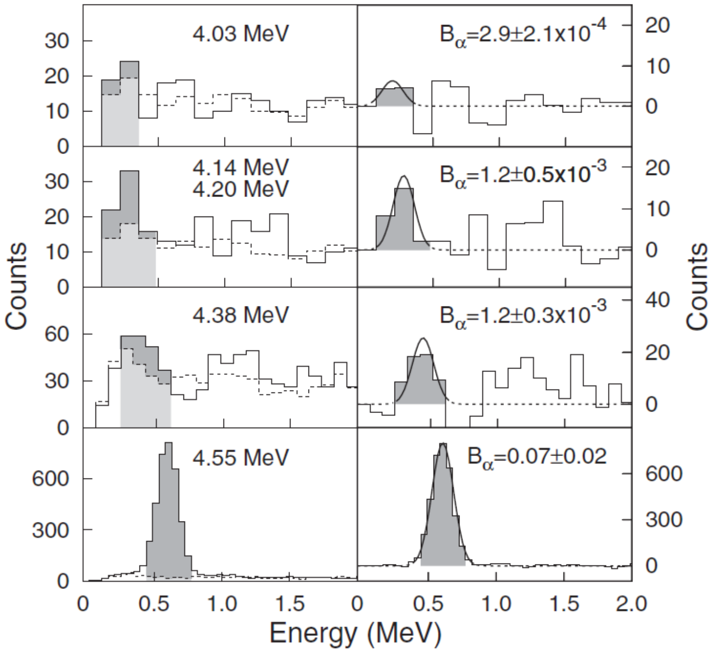


Left:
- Solid (all coincidences)
- Dashed (background)

Right:
- Backgound subtracted

# Branching ratio results



W. P. Tan+ (2007, 2009)

## Triton energy spectrum (single)

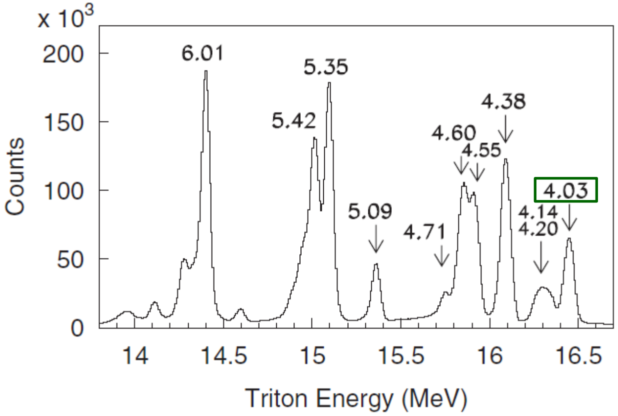


## $\alpha$-t angular correlation

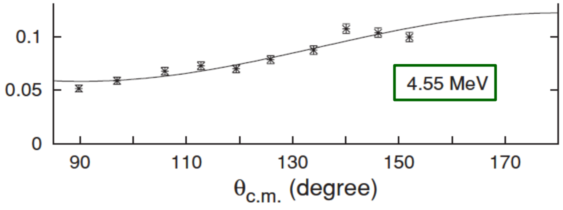


$$W(\theta_{c.m.}) = \frac{1}{4\pi}\sum_{k=0}^{k_{max}} a_{2k}P_{2k}(cos(\theta_{c.m.}))$$

## $\alpha$-particle energy spectrum ($\alpha$-t coincidence)

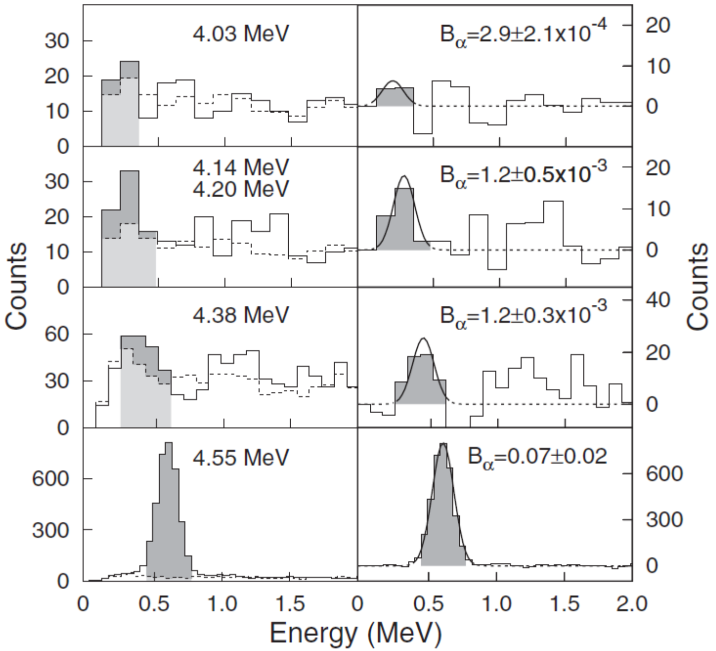


Left:
- Solid (all coincidences)
- Dashed (background)

Right:
- Backgound subtracted

- $B_\alpha$ (4.033 MeV) = 2.9 ± 2.1 x $10^{-4}$
- Compatible with previous upper limits
- Very low statistics (6 $t$-$\alpha$ on 20 background) with $B_\alpha$ compatible with 0 at the 2$\sigma$ level

# The $^7$Li($^{15}$O,t)$^{19}$Ne α-particle transfer reaction



Transfer reactions are a privileged tool to determine partial widths

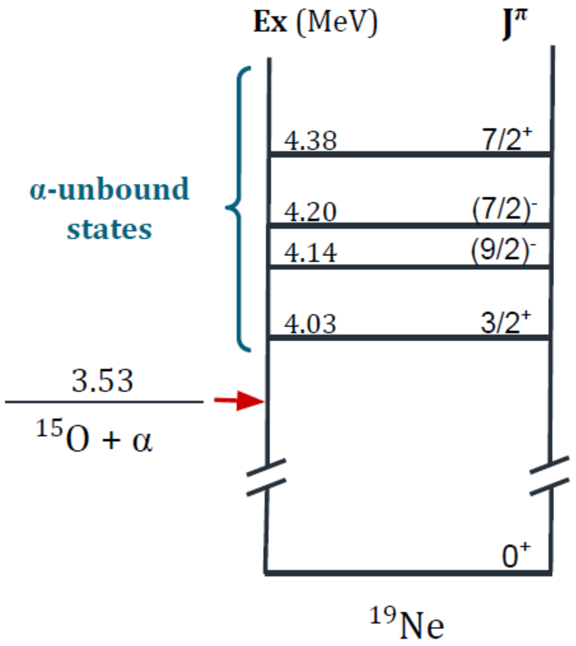


- α-particle transfer reaction commonly use **($^7$Li,t) reactions [$^7$Li = α + t]**
- **Inverse kinematics** since $^{15}$O is radioactive ($T_{1/2}$ = 122 s)

  [not possible to produce targets]

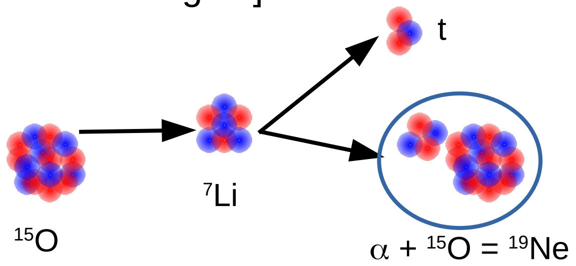


- Comparison between experimental and theoretical differential cross-section

$$\left(\frac{d\sigma}{d\Omega}\right)_{exp} = C^2 S_\alpha \left(\frac{d\sigma}{d\Omega}\right)_{DWBA}$$

- α-particle partial width: $\Gamma_\alpha = C^2 S_\alpha \times \Gamma_\alpha^{s.p.}$ → Theoretical calculation

# The MUGAST + VAMOS + AGATA set-up



J. Sanchez Rojo (2022 PhD)

$^{7}$Li($^{15}$O,t)$^{19}$Ne* → $\gamma$ + $^{19}$Ne$_{g.s.}$

**$^{15}$O @ 4.7 MeV/u**
- ~ 2x10$^{7}$ pps
- SPIRAL1 beam
- $^{15}$N contaminant < 0.5 %

$^{7}$LiF target
1.25 mg/cm$^{2}$
+ $^{nat}$C 20 $\mu$g/cm$^{2}$

# The MUGAST + VAMOS + AGATA set-up



J. Sanchez Rojo (2022 PhD)

$^{7}$Li($^{15}$O,t)$^{19}$Ne* → γ + $^{19}$Ne$_{g.s.}$

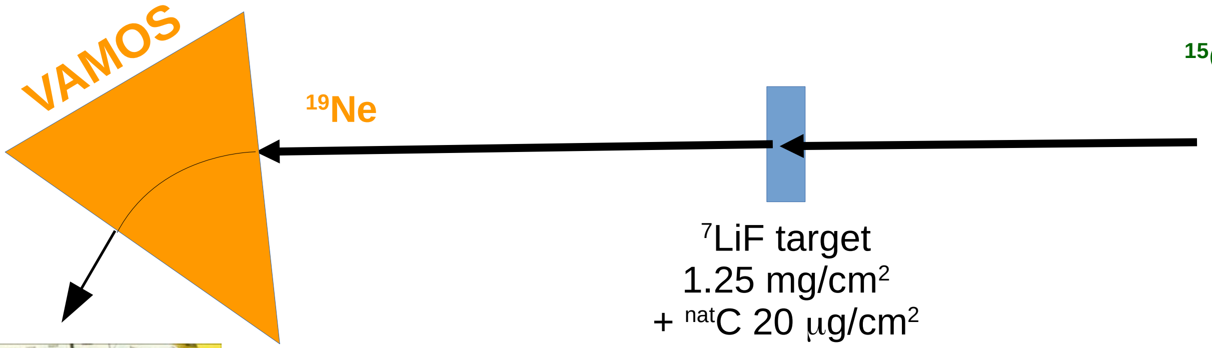


**$^{15}$O @ 4.7 MeV/u**
- ~ 2x10$^{7}$ pps
- SPIRAL1 beam
- $^{15}$N contaminant < 0.5 %

**VAMOS @ 0°**
- ΔΘ ± 7°
- ΔBρ ± 10%

# The MUGAST + VAMOS + AGATA set-up



J. Sanchez Rojo (2022 PhD)

$^{7}$Li($^{15}$O,t)$^{19}$Ne* → $\gamma$ + $^{19}$Ne$_{g.s.}$

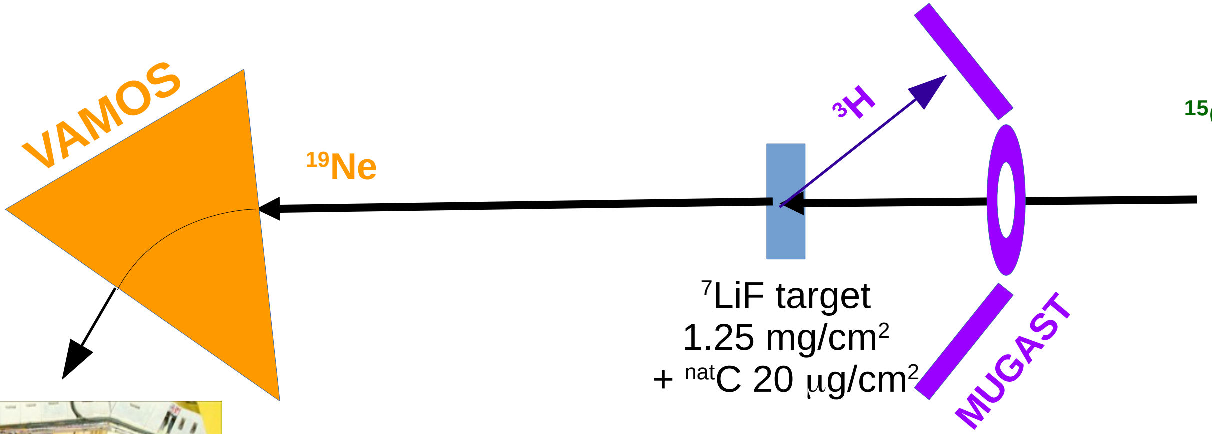


**$^{15}$O @ 4.7 MeV/u**

- ~ 2x10$^{7}$ pps
- SPIRAL1 beam
- $^{15}$N contaminant < 0.5 %

**VAMOS @ 0°**

- $\Delta\Theta$ ± 7°
- $\Delta B\rho$ ± 10%

**MUGAST**

- DSSSD 500 μm
- Trapezoid (x5), annular (x1), square (x2)
- 128+128 strips

# The MUGAST + VAMOS + AGATA set-up



J. Sanchez Rojo (2022 PhD)

$^{7}Li(^{15}O,t)^{19}Ne^{*} \rightarrow \gamma + {}^{19}Ne_{g.s.}$

GANIL spiral2 laboratoire commun CEA/DRF CNRS/IN2P3

**AGATA @ 18 cm**

- 37 crystals
- ε(1 MeV) ~ 8% w/ add-back

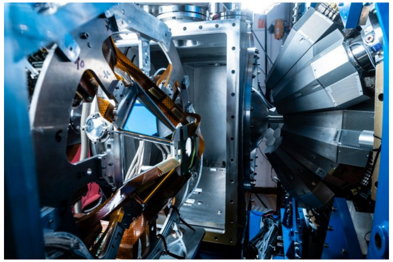

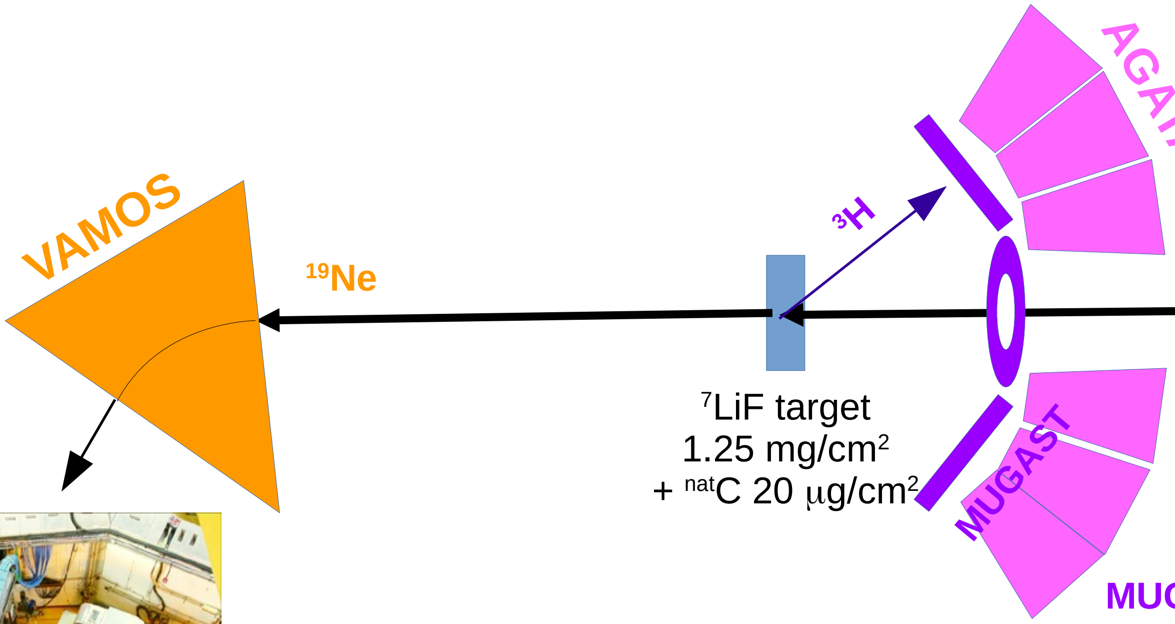


**$^{15}O$ @ 4.7 MeV/u**

- ~ $2 \times 10^{7}$ pps
- SPIRAL1 beam
- $^{15}N$ contaminant < 0.5 %

**MUGAST**

- DSSSD 500 μm
- Trapezoid (x5), annular (x1), square (x2)
- 128+128 strips

**VAMOS @ 0°**

- ΔΘ ± 7°
- ΔBρ ± 10%

# The MUGAST + VAMOS + AGATA set-up



J. Sanchez Rojo (2022 PhD)

$^{7}$Li($^{15}$O,t)$^{19}$Ne* → γ + $^{19}$Ne$_{g.s.}$

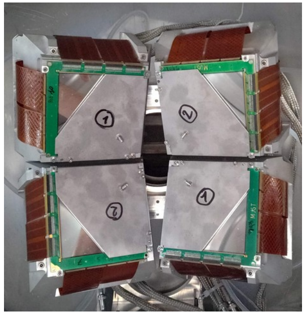

**MUST2**

- DSSSD 300 μm + CsI
- 128+128 strips (10x10 cm$^2$)

**AGATA @ 18 cm**

- 37 crystals
- ε(1 MeV) ~ 8% w/ add-back

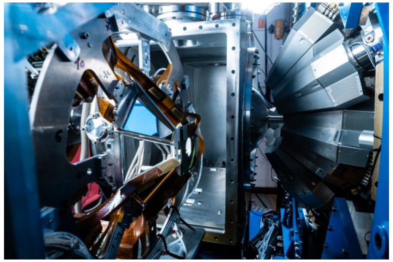

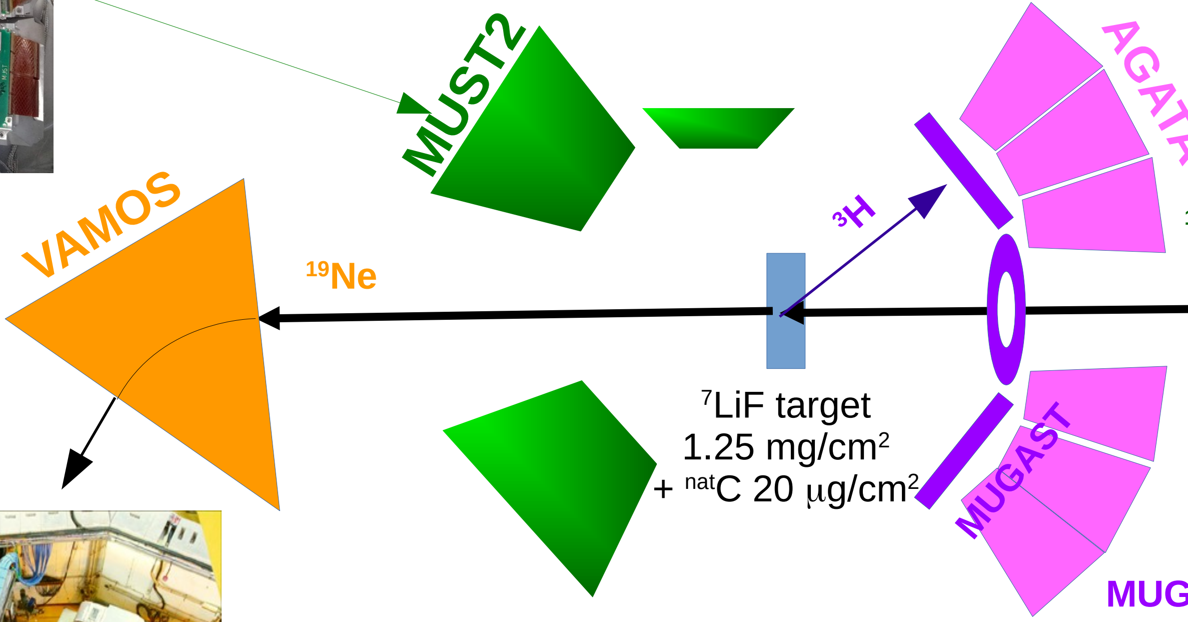


**$^{15}$O @ 4.7 MeV/u**

- ~ 2x10$^7$ pps
- SPIRAL1 beam
- $^{15}$N contaminant < 0.5 %

**VAMOS @ 0°**

- ΔΘ ± 7°
- ΔBρ ± 10%

**MUGAST**

- DSSSD 500 μm
- Trapezoid (x5), annular (x1), square (x2)
- 128+128 strips

# Particle identification



J. Sanchez Rojo (2022 PhD)

- VAMOS spectrometer (recoils)
  - Good selectivity of recoils: A, Z, Q
  - $^{19}$Ne well identified
  - Crucial for background rejection

- MUGAST (light ejectiles)
  - Identification of tritons
  - Crucial for angular distribution

- AGATA (γ-rays)
  - Very good selectivity
  - High energy resolution (after Doppler correction)

    → FWHM 10 keV (@ 1 MeV); 40 keV (@ 4 MeV)

Light ejectiles (MUGAST)

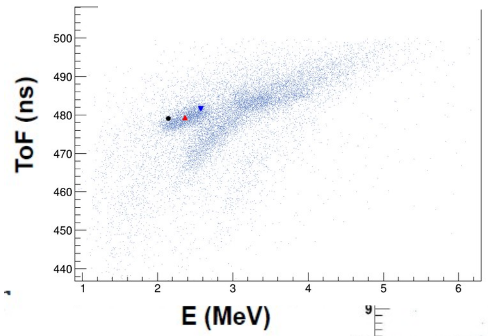


Recoils (VAMOS)

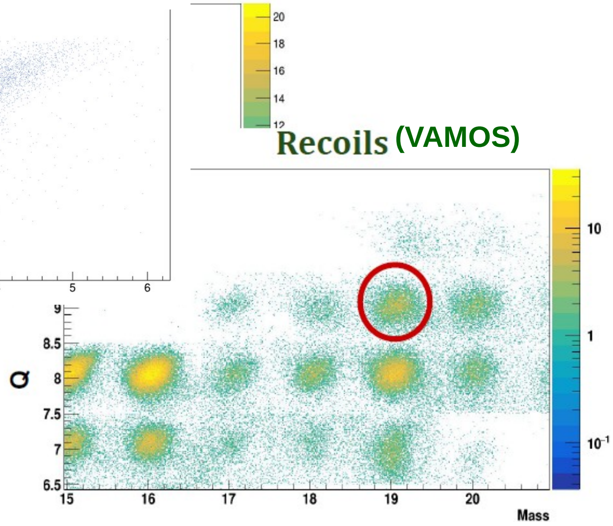


γ-rays (AGATA)

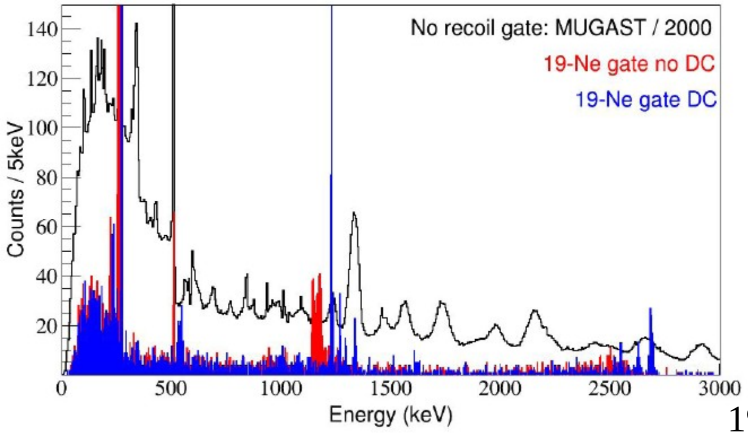

# $^{19}$Ne – t – γ triple coincidences



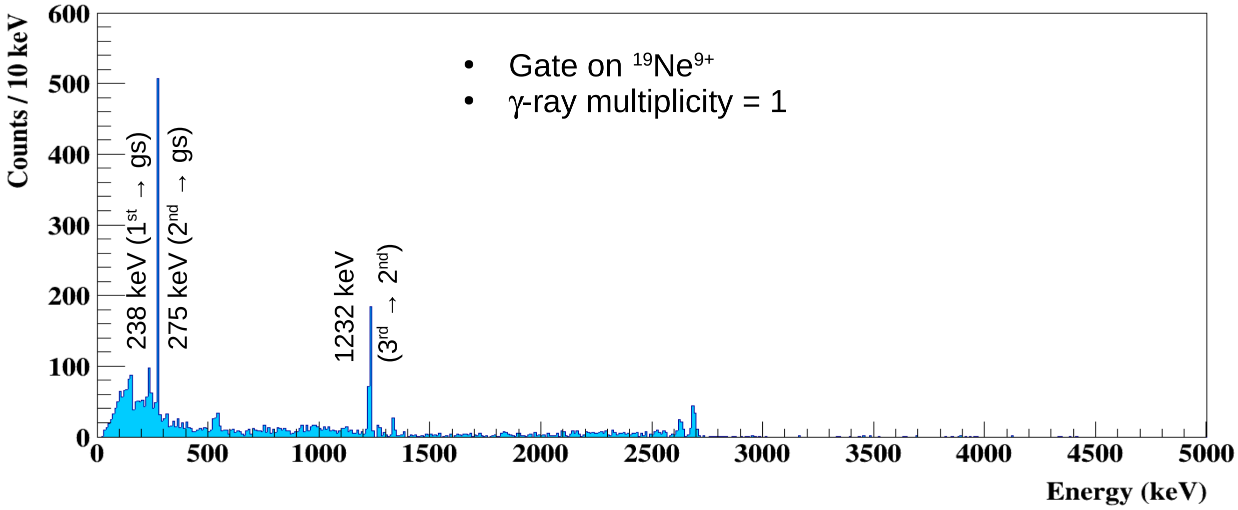

# $^{19}$Ne – t – γ triple coincidences



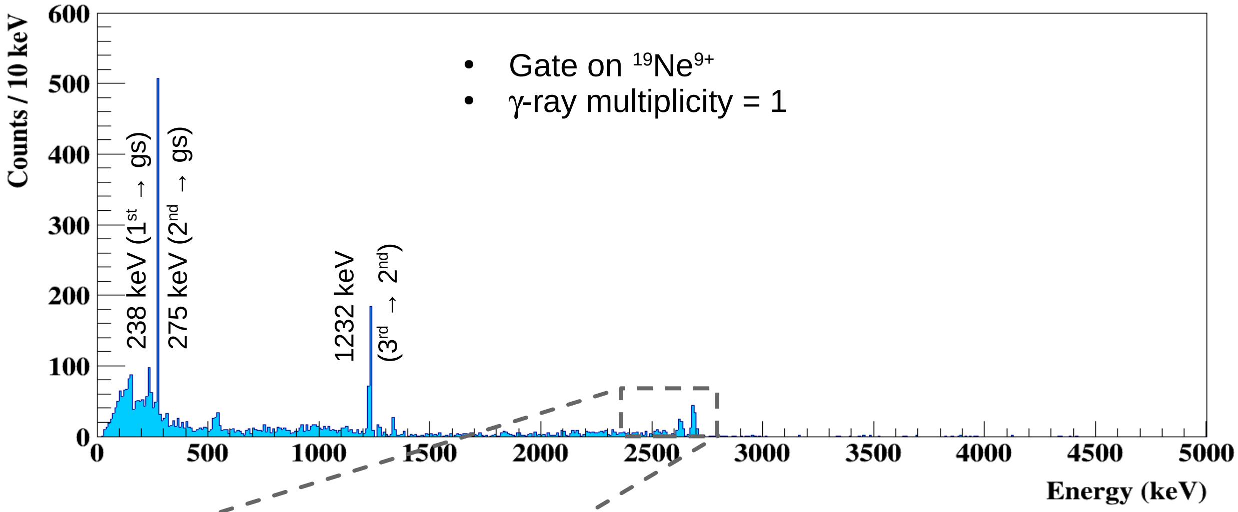


γ-ray transitions from the doublet at 4140 keV and 4197-keV

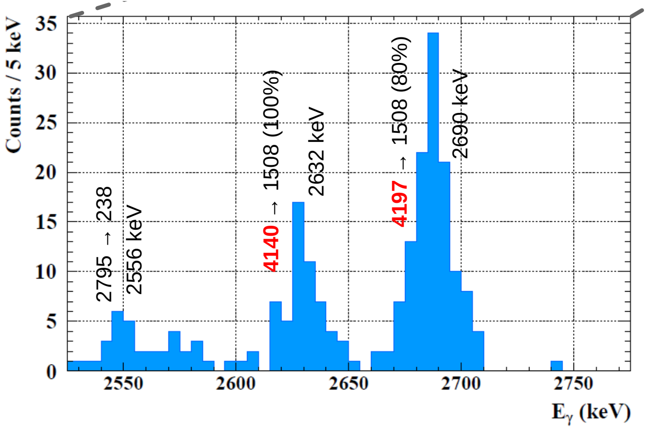

# $^{19}$Ne – t – γ triple coincidences



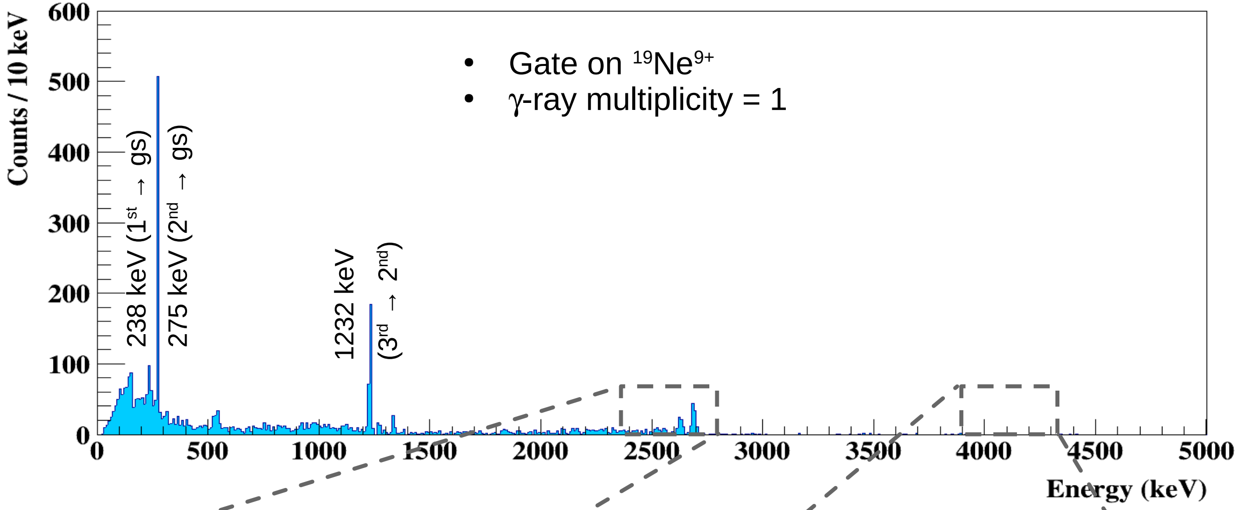


γ-ray transitions from the doublet at 4140 keV and 4197-keV

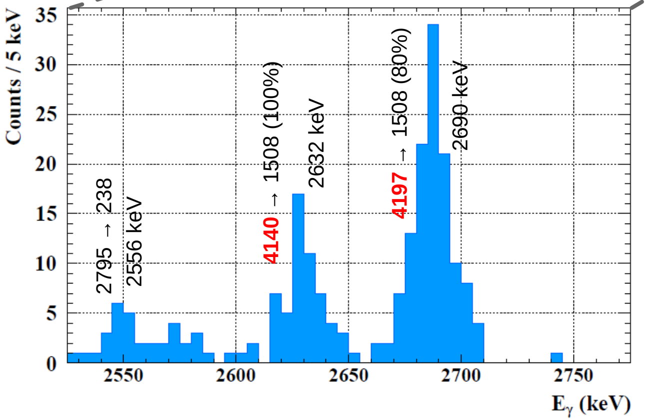


4033 keV state: $N = 2.2^{+2.9}_{-1.6}$ ($1\sigma$ CL)

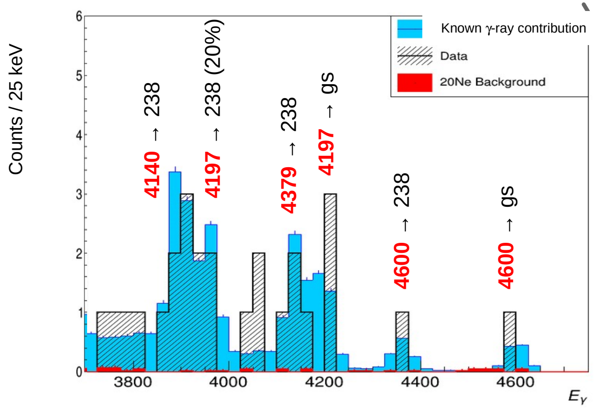


Source of background

- Compton events from high-energy γ-ray lines
- Small leaking (2.3%) of $^{20}$Ne in VAMOS $^{19}Ne^{9+}$ selection

# $^{19}$Ne – t – γ triple coincidences



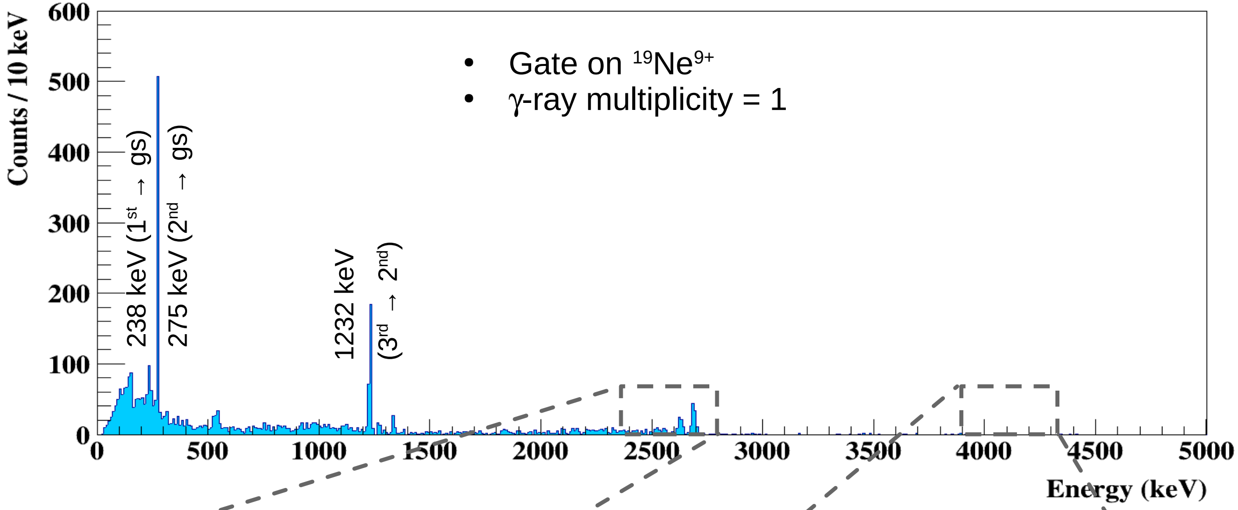


γ-ray transitions from the doublet at 4140 keV and 4197-keV

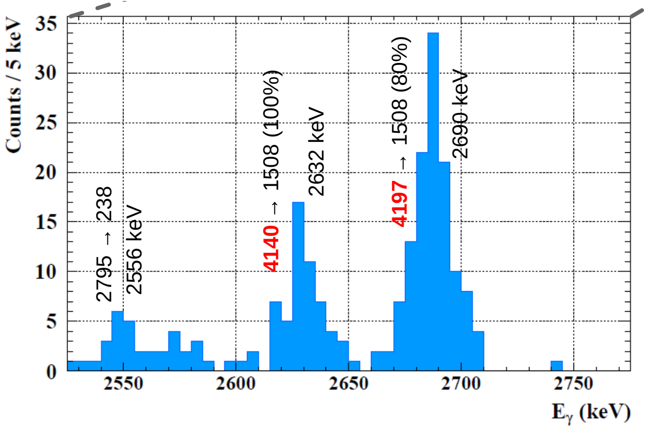


4033 keV state: $N = 2.2^{+2.9}_{-1.6}\ (1\sigma\ \mathrm{CL})$

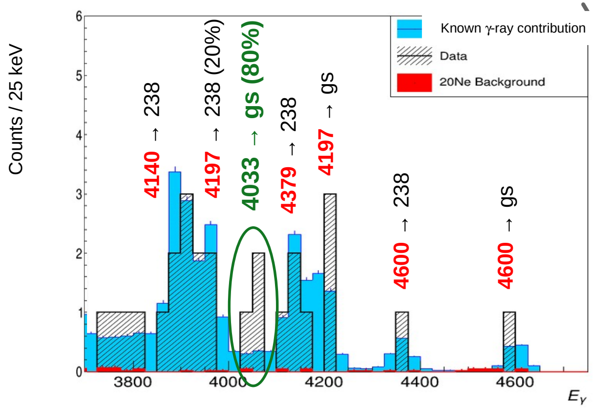


Source of background

- Compton events from high-energy γ-ray lines
- Small leaking (2.3%) of $^{20}$Ne in VAMOS $^{19}Ne^{9+}$ selection

# Angular distributions and $\alpha$ spectroscopic factors



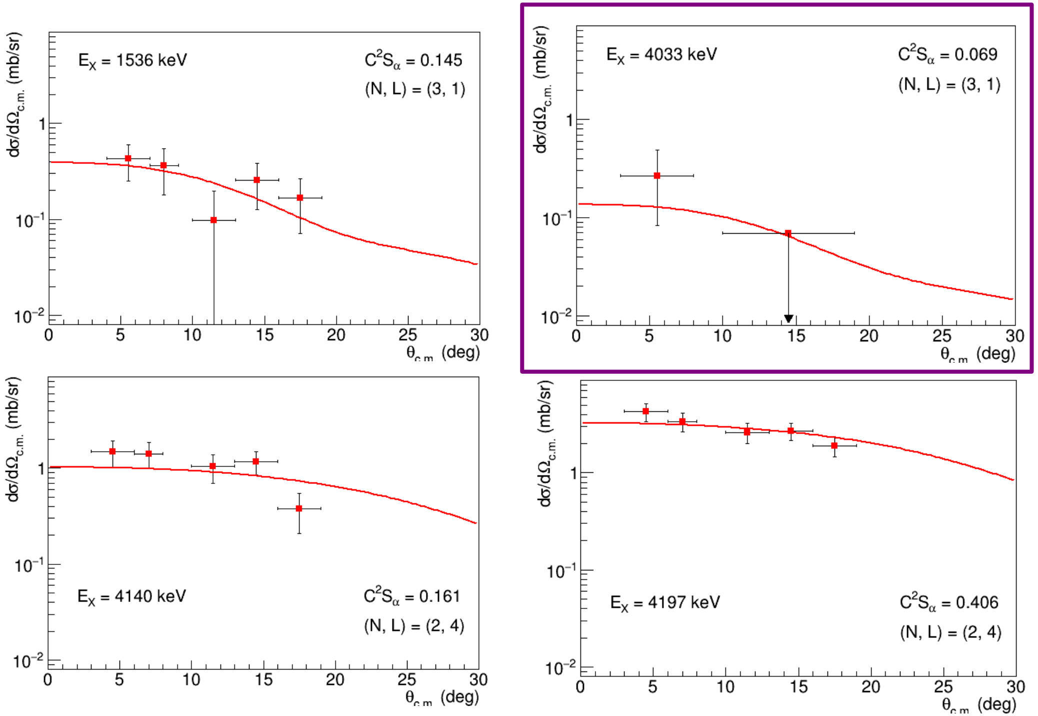


## Comparison with analog states in $^{19}$F

Preliminary

| | | $^{19}$Ne | | $^{19}$F | |
|---|---|---|---|---|---|
| $J^{\Pi}$ | Q=2N+L | $E_x$ (keV) | $C^2S_\alpha$ | $E_x$ (keV) | $C^2S_\alpha$ [a] |
| 5/2- | 8 | 1508 | **0.25** | 1346 | 0.20 |
| 3/2+ | 7 | 1536 | **0.15** | 1554 | 0.21 |
| 3/2- | 8 | 1615 | **0.23** | 1459 | 0.20 |
| 9/2+ | 7 | 2794 | **0.22** | 2780 | 0.16 |
| 3/2+ | 7 | **4033** | **0.063** | 3908 | ≤ 0.09 |
| (7/2-) | 8 | 4140 | **0.16** | 3999 | 0.29 |
| (9/2-) | 8 | 4197 | **0.41** | 4033 | |
| 7/2+ | 7 | 4379 | | 4378 | |
| | | 4549 | | 4556 | |
| (5/2+) | 7 | 4600 | | 4550 | |

[a] F. de Oliveira Santos et al. (1996)

## FR-DWBA analysis (FRESCO)

- Optical potentials from mirror reaction: $^{15}$N(Li,t)$^{19}$F
  F. de Oliveira Santos et al. (1996)
- $C^2S_\alpha$ determination: prescription from Becchetti+ (1978)
  - $L \geq 2$: $\alpha$-cluster bound by 50 keV
  - $L < 2$: $C^2S_\alpha$ extrapolation to actual $\alpha$-separation energy
- Uncertainty due to optical potential ~ 40%

- Good agreement with analog states
- Small $C^2S_\alpha$ for the $E_x$($^{19}$Ne) = 4033 keV state
- $C^2S_\alpha$ determined for the 2 components of the $E_x$($^{19}$Ne) = 4140 + 4197 keV doublet

# α-particle partial widths in $^{19}$Ne



## Determination of $\Gamma_\alpha$ for $^{19}$Ne unbound states

- $\Gamma_\alpha = 2P_l(r, E_r)\frac{\hbar^2 r}{2\mu}C^2 S_\alpha|\phi(r)|^2$
- Radius determined when asymptotic behavior of α + $^{15}$O radial wave function is reached

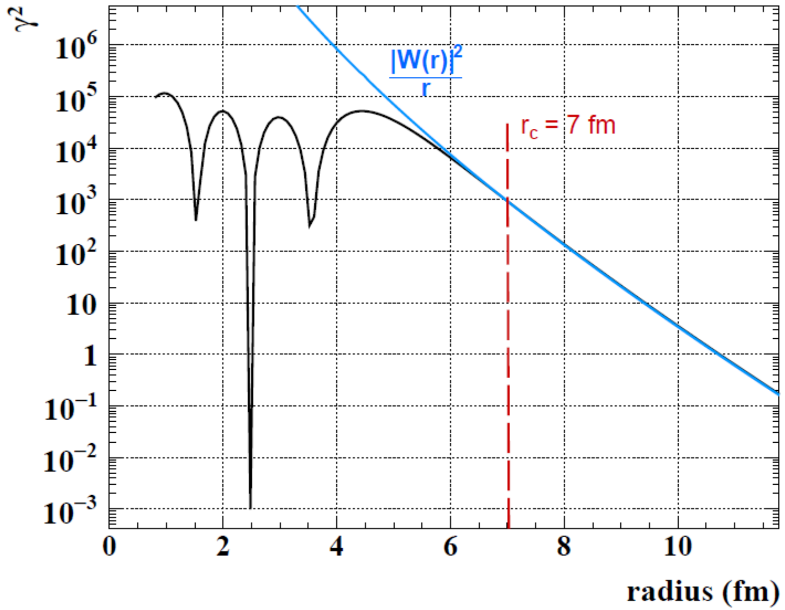


## Comparison with existing data    Preliminary

| | Present work | | Tan+ (2009) | | | Fortune+ (2010) | |
|---|---|---|---|---|---|---|---|
| $E_X$ (keV) | $\Gamma_\alpha$ (μeV) | $B_\alpha$ (x $10^{-4}$) | $\Gamma_\alpha$ (μeV) | $B_\alpha$ (x $10^{-4}$) | τ (fs) | $\Gamma_\alpha$ (μeV) | τ (fs) |
| 4033 | **11.0 (4.4)** | | **17 (13)** | 2.9 (2.1) | $13^{+9}_{-6}$ | **24 (18)** | 7.9 (1.5) |
| 4140 | **1.0 (0.4)** | 0.3 + | **44 (20)** | **12 (5)** | $18^{+2}_{-3}$ | | |
| 4197 | **12.6 (5.2)** | 8.2 | **18 (9)** | | $43^{+12}_{-9}$ | | |

- 4033 keV state: $\Gamma_\alpha$ = 10.8 ± 4.3 μeV
  (uncertainty from DWBA only so far)
- 4140 keV + 4197 keV doublet
  → α-particle partial width for each component

compatible with existing results **BUT** obtained from a direct determination of the α-particle width

1. Generalities
2. Break out of the hot CNO cycle
   a) The $^{15}O(\alpha,\gamma)^{19}Ne$ reaction
   b) The $^{18}Ne(\alpha,p)^{21}Na$ reaction
3. The αp-process and the $^{35}K(p,\gamma)^{36}Ca$ reaction

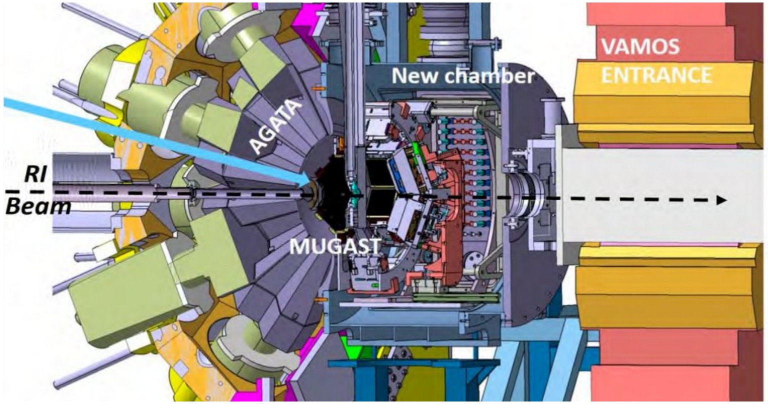


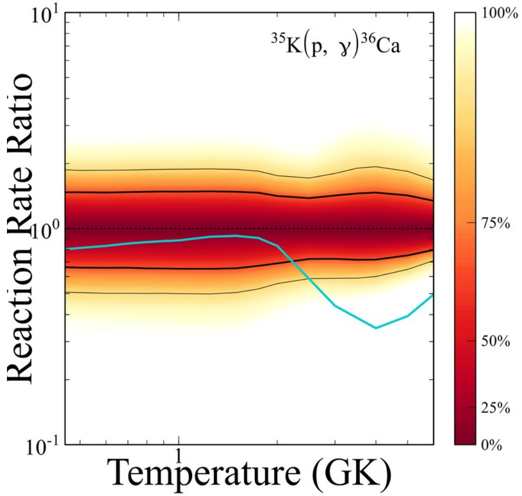

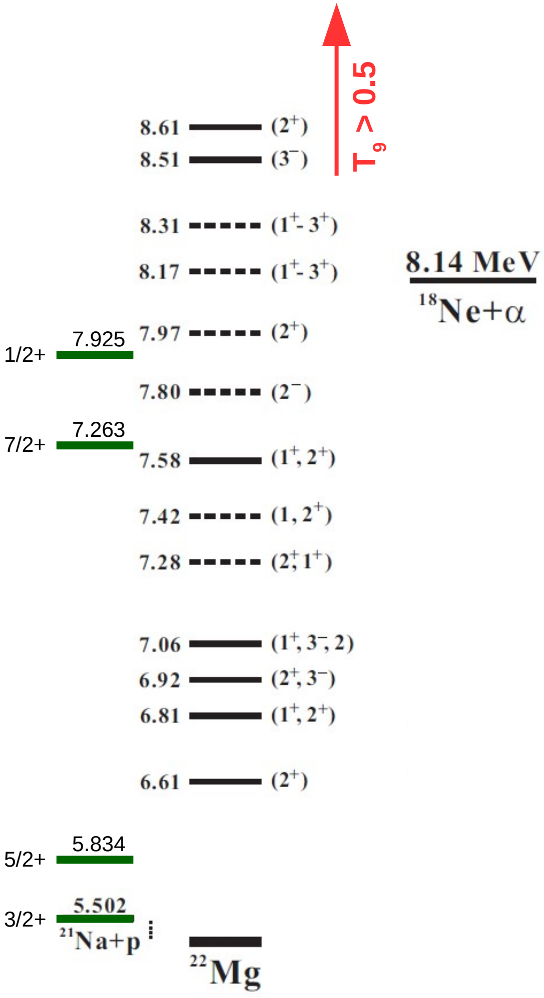


J. He+ EPJA (2008)

## Experimental status

- Activation of $^{18}$Ne(α,p)$^{21}$Na for T > 500 MK
  → $E_x$($^{22}$Mg) > 8.5 MeV
  → $E_{c.m.}$ > 0.5 MeV
- Direct (α,p) measurement extremely challenging close to α-particle threshold (large barrier)
- Determination of nuclear properties of states in compound $^{22}$Mg nucleus [$\Gamma_\alpha$ from analog $^{22}$Ne states or assuming $\langle\theta^2_\alpha\rangle$]

[Giesen+ NPA (1994), Mohr+ PRC (2014)]

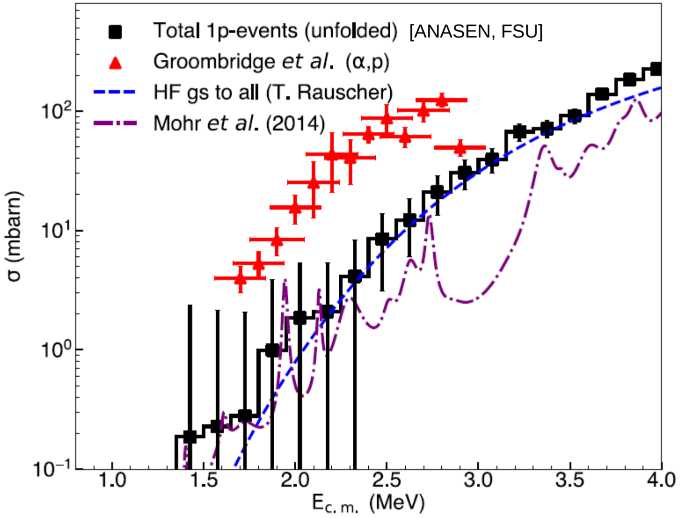


Anastasiou+ PRC (2022)

- High level density ~ 1 state / 125 keV, but only 3 $L$ = 0 and 4 $L$ = 1 states within 3 MeV

# $^{18}$Ne(α,p)$^{21}$Na: status & future experiment

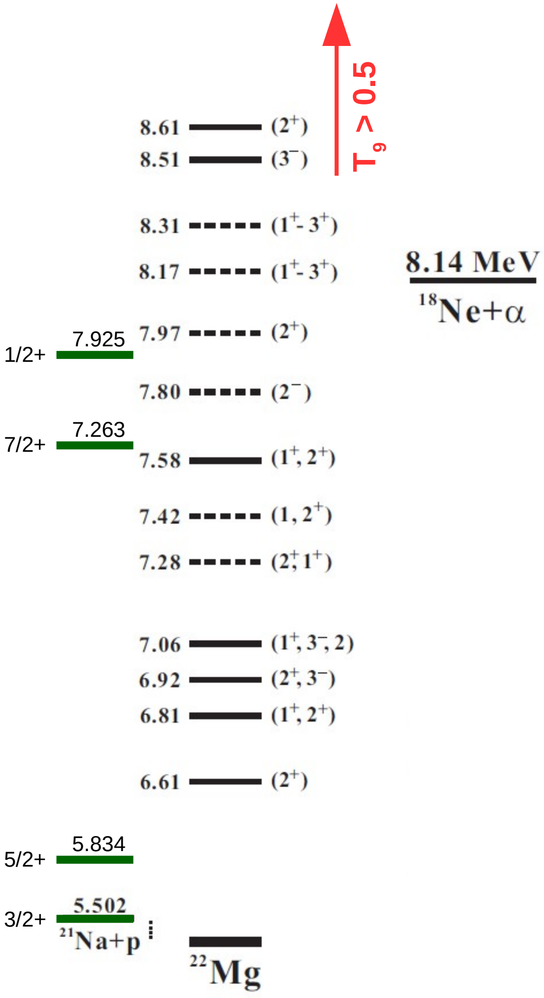


J. He+ EPJA (2008)

## Experimental status

- Activation of $^{18}$Ne(α,p)$^{21}$Na for T > 500 MK
  → $E_x$($^{22}$Mg) > 8.5 MeV
  → $E_{c.m.}$ > 0.5 MeV
- Direct (α,p) measurement extremely challenging close to α-particle threshold (large barrier)
- Determination of nuclear properties of states in compound $^{22}$Mg nucleus [$\Gamma_\alpha$ from analog $^{22}$Ne states or assuming $\langle\theta_\alpha^2\rangle$]

[Giesen+ NPA (1994), Mohr+ PRC (2014)]

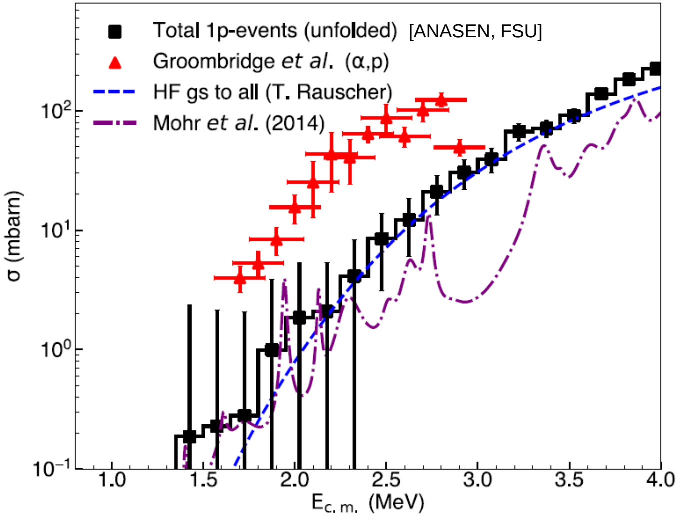


Anastasiou+ PRC (2022)

- High level density ~ 1 state / 125 keV, but only 3 $L$ = 0 and 4 $L$ = 1 states within 3 MeV

## Resonance strength determination

$$\omega\gamma = \omega\frac{\Gamma_\alpha\Gamma_p}{\Gamma} = \omega\Gamma_\alpha \times \mathrm{BR_p}$$

- α-particle transfer reaction (inverse kinematics)
  → resonant $^{22}$Mg states with strong coupling to the alpha channel ($E_x$, $\Gamma_\alpha$)
- Proton decay measurement → **$\mathrm{BR_p}$**
- $^{21}$Na* prompt-decay γ-ray → $p_0$ vs $p_1$ decay channels

# $^{18}$Ne(α,p)$^{21}$Na: study with MUGAST + EXOGAM + ZDD

MUGAST + EXOGAM + ZDD @ LISE

laboratoire commun CEA/DRF spiral2 CNRS/IN2P3

$^{7}$Li($^{18}$Ne,t)$^{22}$Mg(p)$^{21}$Na*(γ)$^{21}$Na$_{g.s.}$

Scheduled in next MUGAST 2025 campaign

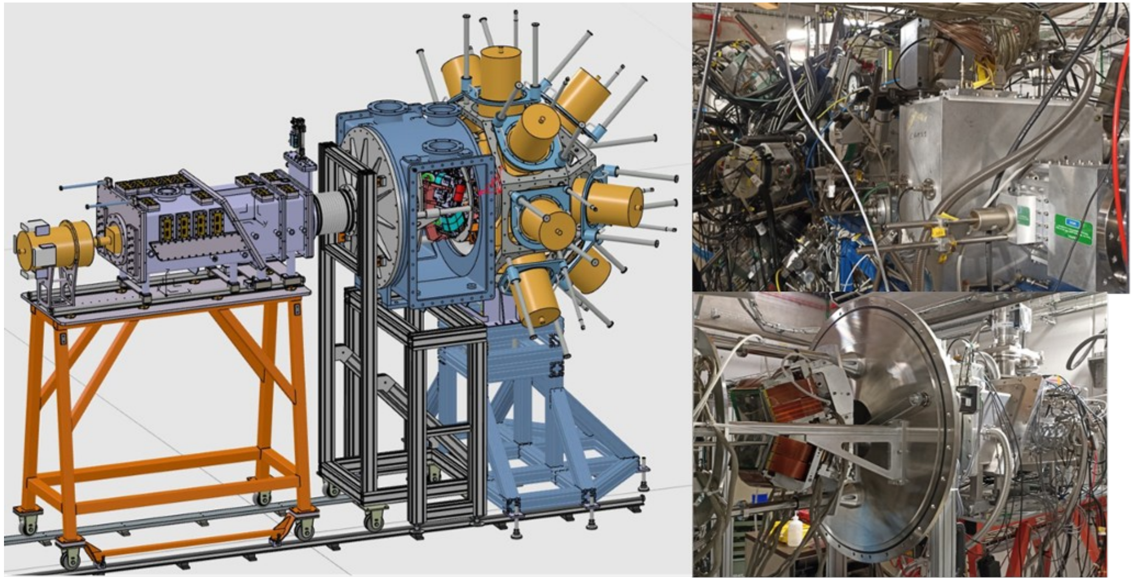

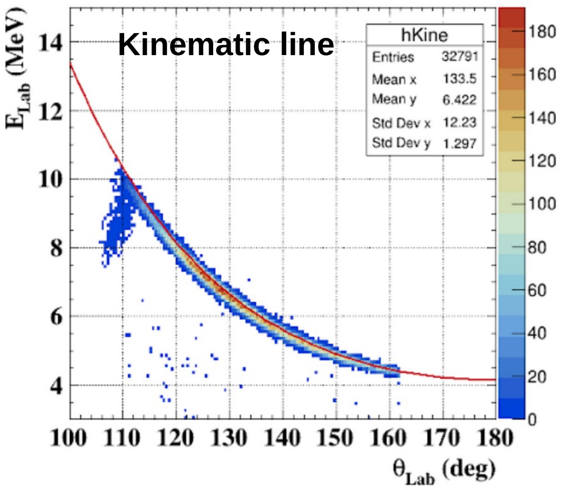


- RIB: $^{18}$Ne @ 5 MeV/u
- Beam intensity: ~ $10^6$ pps
- Target: $^{7}$LiF of ~ 500 μg/cm$^2$

- Triple coincidence using:
  - MUGAST
    - Trapezoids: tritons
      → $E_X$: 560 keV (FWHM)
    - MUST2: proton emission
  - ZDD (modified version):
    - $^{18}$Ne (5 MeV/u) and $^{21}$Na recoil (3.3 MeV/u)
  - EXOGAM: prompt γ-rays (mainly $E_\gamma$ ~ 332 keV)

# Outline

1. Generalities

2. Break out of the hot CNO cycle

   a) The $^{15}O(\alpha,\gamma)^{19}Ne$ reaction

   b) The $^{18}Ne(\alpha,p)^{21}Na$ reaction

3. The $\alpha$p-process and the $^{35}K(p,\gamma)^{36}Ca$ reaction

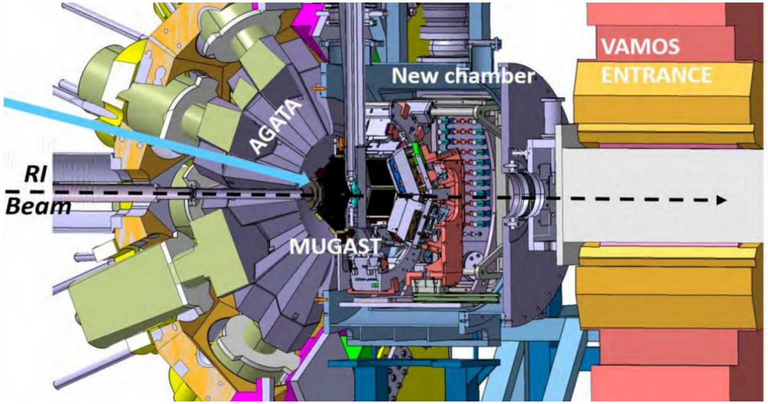


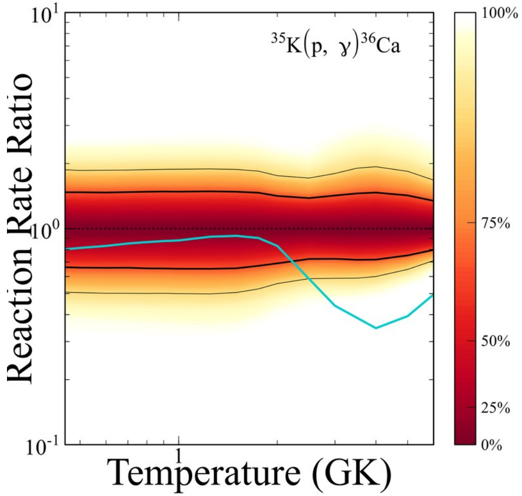

# The αp-process and the $^{35}$K(p,γ)$^{36}$Ca reaction

**(α,p) process**: (α,p) (p,γ) reactions
→ up to A < 60 (radioactive nuclides)
→ impact on energetics and light curve

10 most impacting (p,γ) reactions
(close to waiting points)

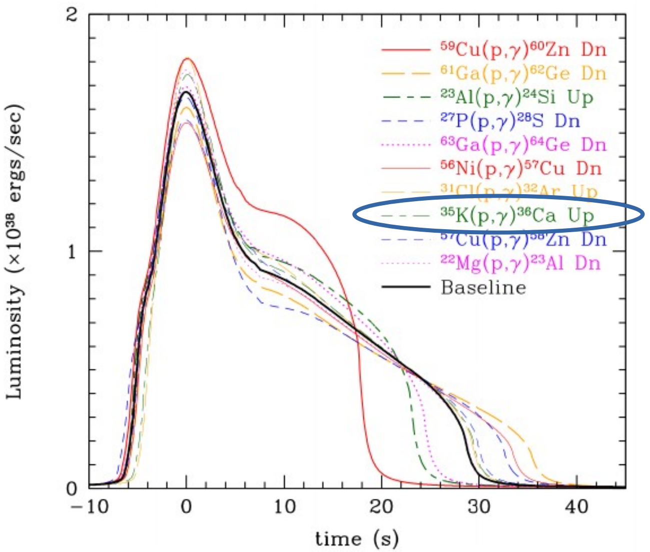


Cyburt+ 2016

$^{34}$Ar waiting point

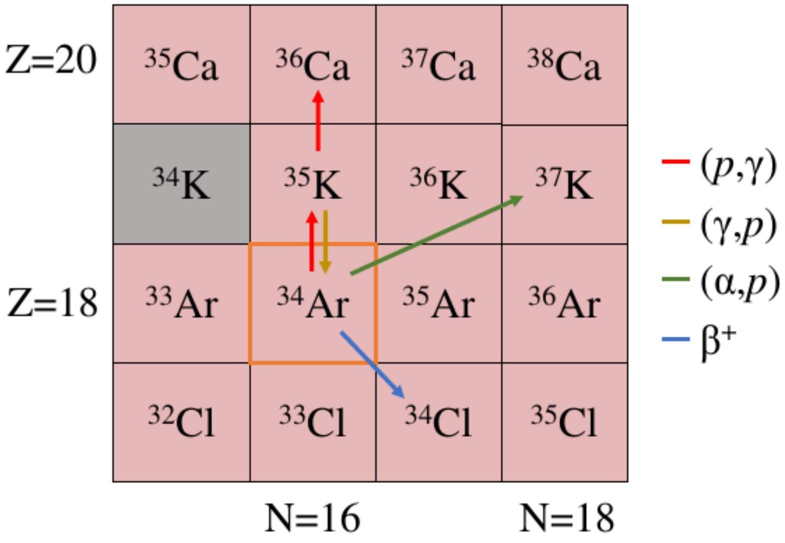


- Small $^{34}$Ar(p,γ)$^{35}$K Q-value [= 80 keV]
  → (p,γ) (γ,p) equilibrium
- $^{34}$Ar(α,p)$^{37}$K must be faster then $^{34}$Ar β-decay ($T_{1/2}$ = 846 ms)
- Other possibility: **$^{35}$K(p,γ)$^{36}$Ca**

# The $^{35}K(p,\gamma)^{36}Ca$ reaction

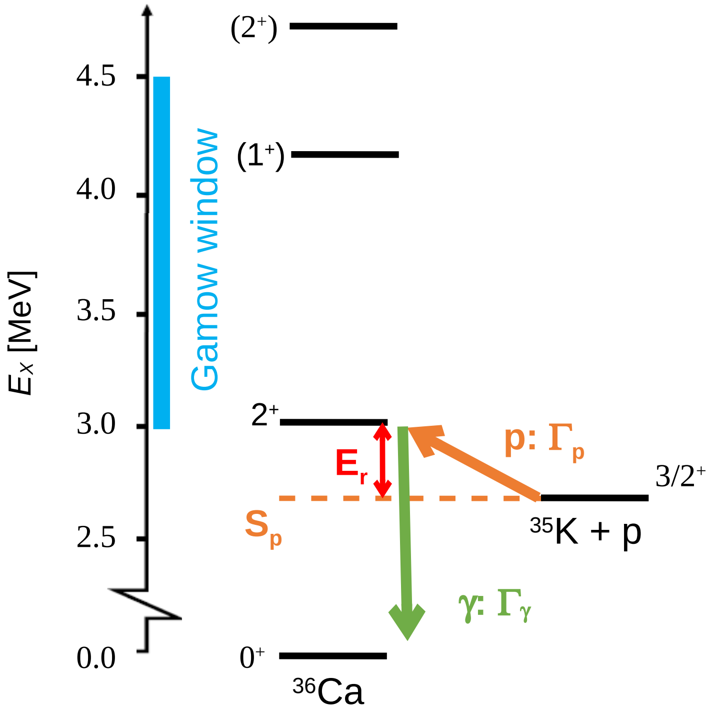


Gamow window: X-ray burst temperature ~ 0.5 – 2 GK

- $^{36}$Ca excitation energy: 3.0 – 4.5 MeV
- $^{35}$K + p resonance energy: 0.4 – 2 MeV

Resonant reaction rate

- $\langle \sigma v \rangle \propto \omega\gamma \times e^{(-E_R/kT)}$ with $\omega\gamma = \frac{2J_R+1}{8} \times \frac{\Gamma_p \Gamma_\gamma}{\Gamma}$, $E_R = E_X - Q_{(p,\gamma)}$

Very limited $^{36}$Ca information available (prior to L. Lalanne's PhD thesis)

- Known first 2+ excitation energy: 3045.0 (2.4) keV
- **BUT** poorly known resonance energy
  → mass excess $\Delta M(^{36}Ca)$ = -6440 **± 40** keV
  (updated value from mass measurement: -6483.6 (56) keV)
  Surbrook+ (2021) PRC
- No partial widths, branching ratios…
- Additional excited states in the Gamow window? Expected from mirror $^{36}$S nuclide

# $^{37}$Ca(p,d)$^{36}$Ca experimental study



**CATS:** Tracking and identification of incoming ions

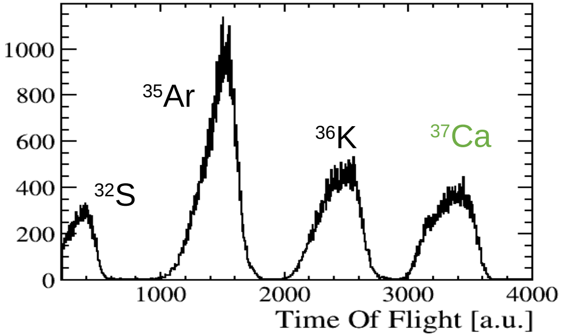


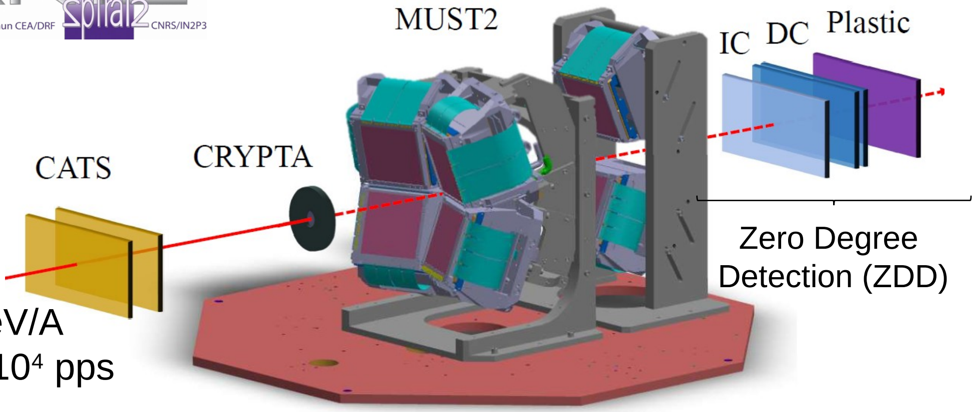


Energy: 48 MeV/A
Intensity: few $10^4$ pps
Purity: 20%

**CRYPTA:** $LH_2$ cryo target

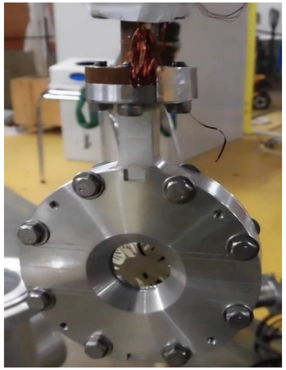

Density:
9 mg/cm$^2$

Thickness:
0.5-1.5 mm

**MUST2:** Light particle id.

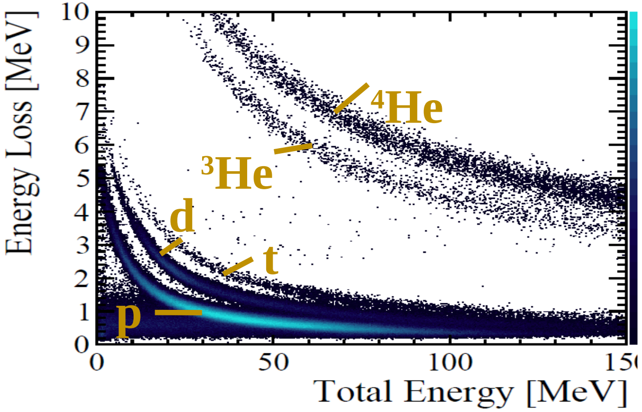


**ZDD:** Outgoing heavy ions id.

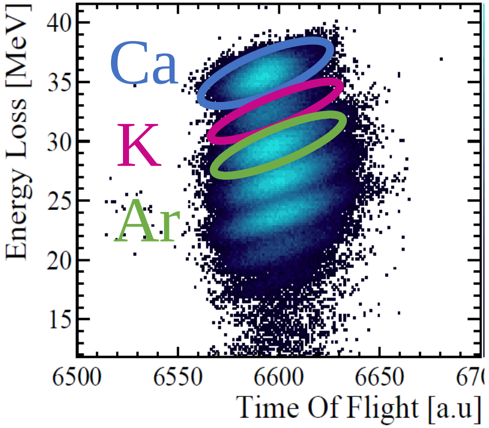

# New $^{36}$Ca states and differential cross-sections

## Excitation energies

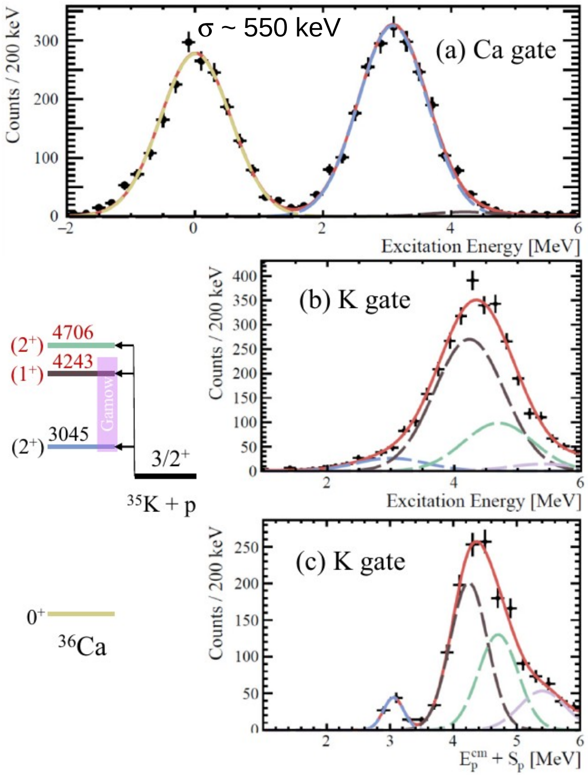


Lalanne+ (2021) PRC

- ΔM($^{36}$Ca) = -6480 (40) keV
- $E_X(2^+)$ = 3057 (20) keV

→ in agreement with previous works

## Differential cross-sections

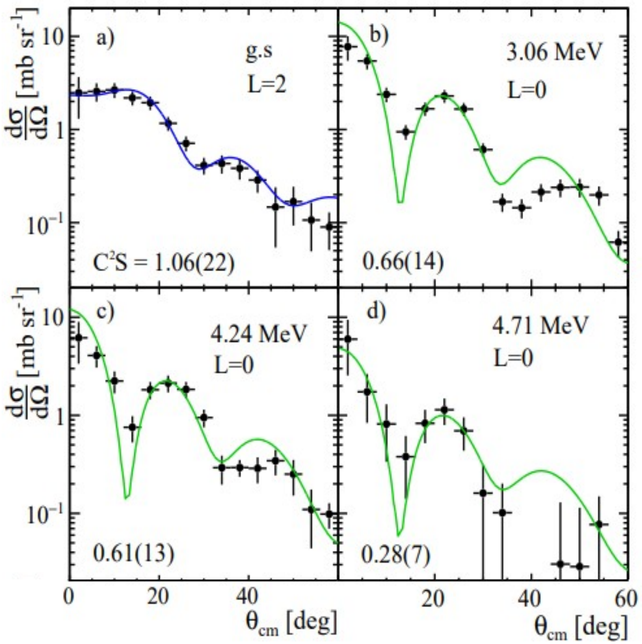


- 2 new $L$ = 0 excited states identified
- Lower one in the Gamow window
- Spin / parity based on analog states in $^{36}$Si and shell-model calculations

# Proton branching ratio ($\Gamma_p/\Gamma$)

## Integral ratio

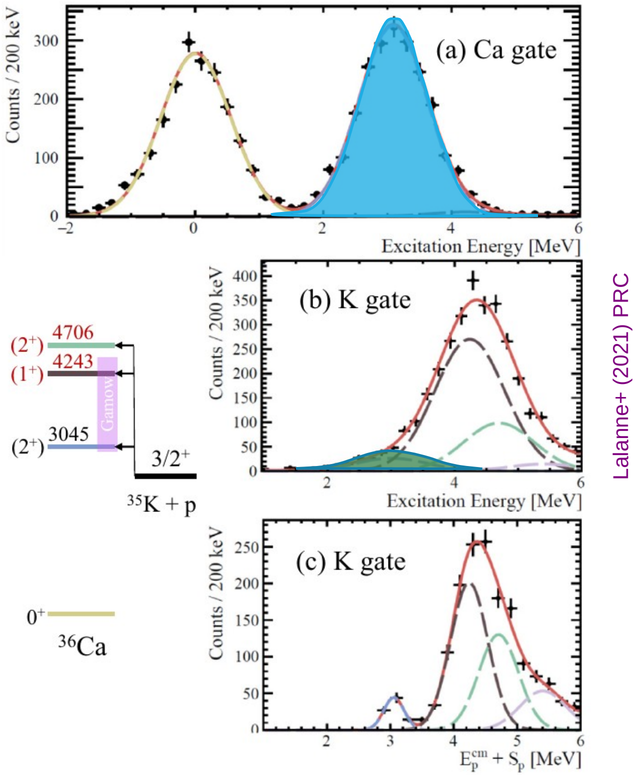


$B_p = 1/(1+\Gamma_\gamma/\Gamma_p)$ with $\Gamma_\gamma/\Gamma_p = N_\gamma / N_p$

$\mathrm{B}_p(2_1^+) = 0.17(2);\ B_p(1^+) > 0.96;\ B_p(2_2^+) > 0.97$

## Angular correlation

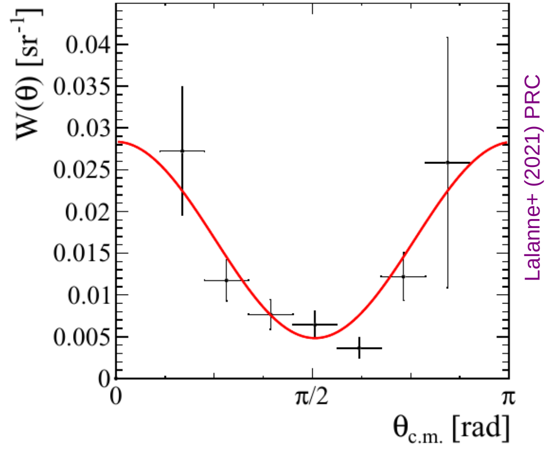


$$W(\theta_{cm}) = \frac{N_{coinc,\Delta\theta}}{N_{single}} \times \varepsilon_{\Delta\theta} \quad \mathrm{sr}^{-1}$$

- 2nd order Legendre polynomial → confirm 2+ spin / parity
- $\mathrm{BR} = \int_{\theta_{cm}=0}^{\pi} 2\pi \sin(\theta_{cm}) W(\theta_{cm}) d\theta_{cm}$

$\mathrm{B}_p(2_1^+) = 0.16(2)$

# The thermonuclear $^{35}K(p,\gamma)^{36}Ca$ reaction rate

## $^{35}K$ + p resonance parameters

| $J^{\pi}$ | $E_r$ (keV) | $\Gamma_\gamma$ (meV) | $\Gamma_p$ (meV) | $\omega\gamma$ (meV) |
|---|---|---|---|---|
| $(2^+)$ | 445(7) | 0.99[a] | 0.20 | 0.102(50) |
| $(1^+)$ | 1643(41) | 65.4[a] | | 25(14) |
| $(2_2^+)$ | 2106(100) | 7.4[a] | | 4.6(25) |

Resonance strength $$\omega\gamma = \frac{2J_R+1}{8} \times \frac{\Gamma_p\Gamma_\gamma}{\Gamma}$$

- γ-ray width ($\Gamma_\gamma$) from *sdpf* shell-model calculations
- Uncertainty of a factor of 1.7 based on other shell-model calculations and mirror state property

## Reaction rates: RatesMC code Longland+ (2010) NPA

Lalanne+ (2021) PRC

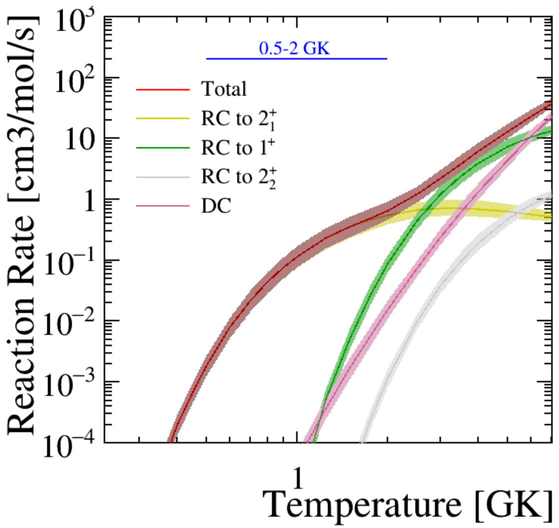


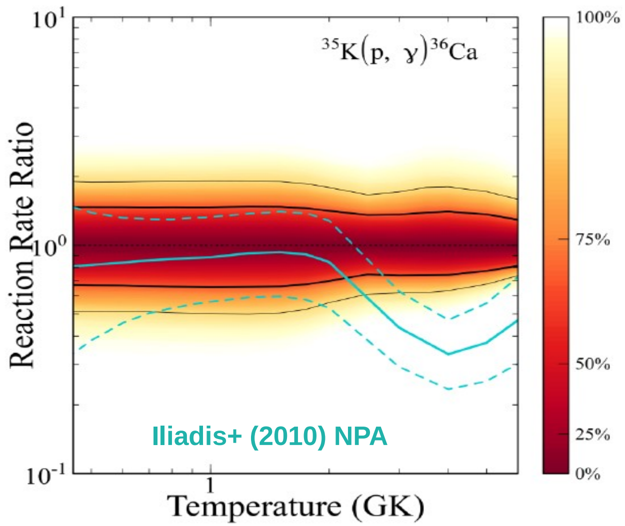


- First 2+ state dominate the reaction rate
- Higher resonant states contribute for T > 2 GK
- In agreement with compilation work from Iliadis+ (2010)

$^{35}K(p,\gamma)^{36}Ca$ sufficiently well constrained
→ no impact on X-ray burst light-curve

# Summary

- Type I X-ray bursts are fascinating objects
  - a few tens of ($\alpha$,p) + (p,$\gamma$) reactions to study

    → relatively far from the valley of stability → mostly radioactive beams

- Several complementary experimental approaches needed for a single reaction

- Indirect methods are a unique tool to determine spectroscopic properties of nuclei of interest (spin/parity, partial width, branching ratios…)

- Few key reactions
  - $^{15}$O($\alpha$,$\gamma$)$^{19}$Ne: very challenging measurement, complementary strength determination welcomed!
  - $^{18}$Ne($\alpha$,p)$^{21}$Na: low-energy cross-section still missing

    → future experiment scheduled soon + other ideas (see C. Fougères' talk)
  - $^{35}$K(p,$\gamma$)$^{36}$Ca now well constrained
  - Other ($\alpha$,p) & (p,$\gamma$) key reactions: $^{59}$Cu(p,$\gamma$)$^{60}$Zn...

# Suggested reading

- **Nuclear astrophysics**
  - ***Nuclear Physics of Stars***, C. Iliadis (2015)

- **Classical novae and type I X-ray bursts**
  - ***Stellar Explosions: Hydrodynamics and Nucleosynthesis***, J. José (2016)

- **Nuclear reaction theory**
  - ***Direct Nuclear Reactions***, G. R. Satchler (1983)

- **Transfer reactions**
  - ***Direct Nuclear Reaction Theories***, N. Austern (1970)
  - ***Transfer reactions as a Tool in Nuclear Astrophysics***, F. Hammache and N. de Séréville (2021)

- **Angular correlations**
  - ***Gamma-ray angular correlations from aligned nuclei produced by nuclear reactions***, A. E. Litherland and J. Ferguson (1961)
  - ***Angular correlations of sequential particle decay for aligned nuclei***, J. G. Pronko and R. A. Lindgren (1972)